Published in : Engineering Structures (2023), 116386
DOI: 10.1016/j.engstruct.2023.116386
Status : Postprint (Author's version)

SEISMIC PRE-QUALIFICATION TESTS OF EC8-COMPLIANT EXTERNAL EXTENDED STIFFENED END-PLATE BEAM-TO-COLUMN JOINTS

Mario D'Aniello

Department of Structures for Engineering and Architecture, University of Naples "Federico II", Via Forno Vecchio 36, 80134 Naples, Italy.

Roberto Tartaglia

Department of Engineering, University of Sannio, Piazza Roma 21, 82100 Benevento, Italy.

Raffaele Landolfo

Department of Structures for Engineering and Architecture, University of Naples "Federico II", Via Forno Vecchio 36, 80134 Naples, Italy.

Jean-Pierre Jaspart

UEE Research Unit, University of Liège, Belgium.

Jean-François Demonceau

UEE Research Unit, University of Liège, Belgium.

Abstract.

An experimental and numerical campaign was carried out to validate the design procedure and prequalify extended stiffened end-plate (ESEP) joints for ductile seismic resistant moment-resisting frames in the framework of Eurocodes. In fact, the tested ESEP joints have been designed with the aim of guaranteeing ductile and dissipative seismic response in accordance with the principles of the hierarchy of resistances to enforce plastic deformations in ductile components of the joints. Two alternative types of dissipation mechanisms are promoted, namely either (i) plastic deformations solely in the connected beam using full strength joints or (ii) plastic deformations in both the beam and the connection using equal strength joints. The adopted design criteria and technological details are described and discussed. The results of experimental tests confirmed the expected yielding mechanisms of the joints, which satisfied the acceptance criteria for both North American and European prequalification. Finite element simulations of ESEP joints have been validated against the experimental results and have been used to investigate the local response of the joints, thus highlighting the influence of both geometrical and mechanical parameters.

Published in : Engineering Structures (2023), 116386
DOI: 10.1016/j.engstruct.2023.116386
Status : Postprint (Author's version)

Keywords. Steel bolted joints, Partially restrained joints, Extended stiffened end-plate connection, Seismic design, Moment-rotation response,FEM analysis.

1. Introduction

Extended stiffened end-plate (ESEP) joints are rather common in European steel moment-resisting structures. In Europe, these joints are currently designed and verified for non-seismic loads according to EN1993-1-8:2005 [1] (hereinafter also referred to as EC3-1-8), which provides criteria for the classification of joints by stiffness and strength, as well as rules to determine resistance and stiffness for analytical modelling of joints. However, limited guidance is provided to guarantee the ductility (i.e., the rotation capacity) of joints, since EN1993-1-8 [1] is covering design under static loading. Guidance to ensure an appropriate joint ductility for plastic analysis is provided, but these rules cover only the case of elastic-perfectly plastic behaviour of members and joints neglecting strain hardening of yielding components and the random variability of their material strength. However, these issues are highly important for seismic-resistant structures. With this regard, EN1998-1 [2] complements EN1993-1-8 [1] by prescribing the following additional requirements:

1) In the case of full strength beam-to-column joints, the design moment resistance of the joints $M_{j,Rd}$ should be greater than 1.1 x γ_{ov} x $M_{b\cdot rd}$, where, 1.1 accounts for the strain hardening, γ_{ov} is the material overstrength factor that accounts for the variability of the yield stress of the steel in the beam (whose recommended value is set equal to 1.25 for all steel grades), and $M_{b\cdot rd}$ is the design bending resistance of the beam.

- 2) In the case of joints with dissipative connections, EN 1998-1 [2] recommends i) to verify that the rotation demand due to the drifts imposed by seismic actions does not exceed the rotation capacity of the joints; (ii) to verify the stability of connected members at the ultimate limit state (ULS); (iii) to ensure that the rotation capacity provided by the beam and its connection (thus without the deformation of the column) is not smaller than 0.035 and 0.025 rad in DCH (i.e. ductility class high) and DCM (i.e. ductility class medium), respectively.
- 3) EN1998-1 [2] requires limiting the rotation of the column web panel to 30% of the overall joint rotation.

However, these requirements do not guarantee the ductile response of the joints, which may experience undesired performance. In fact, the design flexural résistance in accordance with criterion (1) does not ensure the formation of the plastic hinge solely in the beam because of the following issues:

- the actual strain hardening of plastic hinge could be greater than 1.1 (e.g., ductile I-beams with proper torsional restraints experience ultimate moments greater than 1.2 their plastic resistance [3,47]);
- the actual value of the steel yield stress could be higher than 1.25 times the corresponding nominal value [4];
- the plastic hinge form neither in the beam-column axis nor at the column face, therefore the design moment demand evaluated in accordance with criterion (1) underestimates the increase of moment due to shear force in the section where the plastic hinge forms.
- as shown in [5-8,48], the plastic hinge of steel beams under cyclic rotations develops both torsional and out-of-plane bending moments due to the location of flange/web buckling. In the case of ESEP joints, the torsional moments may be more than 10% of the design major axis bending resistance of

the beams, while the minor axis bending moments may reach 22% of the design major axis bending resistance [7]. Therefore, these effects are not accounted for by requirement (1) but may highly affect the resistance of the connection which can experience premature failure due to the severe demand transferred by the plastic hinge if its full ductility has to be exploited.

For what concerns the case of joints with dissipative connection, the requirements summarized by (2) require the rotation capacity to be demonstrated experimentally, thus resulting in unfeasible or expensive projects. As a result, to avoid experimental tests, most designers adopt full strength joints. However, even full strength joints fully compliant with current Eurocodes may not guarantee the required ductility. In fact, both monotonic and cyclic ductility and rotation capacity of plastic hinges in steel beams are affected by the type and the shape of stiffeners/ haunches that may trigger fracture and/or premature buckling thus leading to unfavourable degradation of resistance and rigidity [9-17].

Requirement (3) is judiciously prescribed to limit the distortion of the joints that may trigger damage in the elements connected in the transverse direction (since the actual joints in the buildings are 3D assemblies) as well as to limit the residual drift and the out-of-plumb after severe earthquakes. However, such a requirement cannot be easily accomplished once the column panel zone yields; its post-yield stiffness of the column panel zone is quite low thus favouring the concentration of plastic deformations there.

In light of all these considerations, there is a need to update the EC8 requirements in order to overcome such criticisms. A pragmatic and efficient way to proceed with this aim is the adoption of seismically prequalified joints, guaranteeing specific seismic performance by means of ad-hoc design criteria, verified details, and proofed constructional procedures.

Seismic prequalification of joints is the adopted solution in the United States of America (USA) [18-20] and Japan [21,22]. The Japanese prequalification is mainly addressed for full welded joints made with cold-formed hollow columns, while the North American prequalification covers many other types of bolted connections including the case of ESEP joints. The requirements for US seismically prequalified ESEP joints are given in AISC358 [20] and are mainly based on the studies carried out by [23-26]. In fact, Murray [23] presented design procedures for the eight-bolt extended stiffened end-plate moment connections. Afterward, Sumner and Murray [25,25] carried out an extensive theoretical and experimental campaign to qualify seismically ESEP joints. Their tests demonstrated that this type of bolted joint can satisfactorily guarantee energy dissipation capacity, without appreciable degradation of strength and stiffness. Provided that the beam-to-column hierarchy would be satisfied, the design philosophy was envisioned to provide adequate strength in both the connection and the column web panel to allow the formation of a plastic hinge near the beam extremity.

In 2004, Murray and Sumner [26] presented a unified method for the design of ESEP joints subjected to both wind and seismic loading that uses yield line theory to predict the end-plate and column flange strength. Their findings represent the scientific and technical background of the rules given by current AISC 358-16 [5] for ESEP joints.

Unfortunately, these rules cannot be directly used in Europe because of the following reasons:

- European steel grades differ from North American steel in terms of strength, toughness, and also ductility.

- The shapes of member profiles are different (e.g., the profiles are typically "W" wide flange profiles

Published in : Engineering Structures (2023), 116386
DOI: 10.1016/j.engstruct.2023.116386
Status : Postprint (Author's version)

in the USA, while HE-A, B, and M for European columns and IPE for European beams, etc.).

- The permitted mill imperfections of steel hot-rolled profiles are different in Europe (see EN 10,034 [27]) and USA (see ASTM A6/ A6M [28]), e.g., in USA the out-of-square of the flange tips with respect to the nominal mid-axis of the flange is twice larger than those accepted for European profiles, as shown in [5].
- The type of bolts, welding, and electrodes in Europe differ from those in the USA.
- The philosophy to evaluate the resistance of end-plate connections in Eurocodes is substantially different from US codes. For instance, AISC 358 [20] recommends the yield line method, thus providing equations to estimate the length of the yield line and to determine the associated bending resistance in a closed form for pre-defined configuration of the connections (i.e., for both 4-bolt and 8-bolt rows configuration). On the contrary, EN1993-1-8 [1] adopts the equivalent T-Stub theory, which allows calculating the resistance of an equivalent T-Stub at each active bolt row.

Therefore, specific research projects have been funded within the framework of the European Research Fund for Coal and Steel (RFCS) in order to seismically prequalify different types of bolted beam-to-column joints. These projects are EQUALJOINTS and EQUALJOINTS-Plus (hereinafter referred to as EJ) and more details about the relevant objectives, outcomes, and findings are given in [29].

The results of the experimental tests and corresponding finite element simulations on ESEP joints in EJ projects are summarized and discussed in this article, which is organized into three main parts as follows: (i) the design criteria and technological details of the tested joints; (ii) the experimental program and the obtained results; (iii) the comparison of finite element simulations with experimental results.

2. Design assumptions and technological details

2.1. DESIGN CRITERIA

The adopted design criteria for ESEP joints aim at guaranteeing ductile and dissipative seismic response in accordance with the EN1998- 1 [2] philosophy. Therefore, the principles of hierarchy of resistances are adopted to enforce plastic deformations in ductile components of the joints, thus prioritizing the sequence of yielding of their macro- components (e.g., the web panel, the connection, the beam, and the column as shown in Fig. 1a), and their sub-components (e.g., end-plate, bolts, welds, etc.) as shown in former background studies [5-7,29,30,47-49].

Published in : Engineering Structures (2023), 116386
DOI: 10.1016/j.engstruct.2023.116386
Status : Postprint (Author's version)

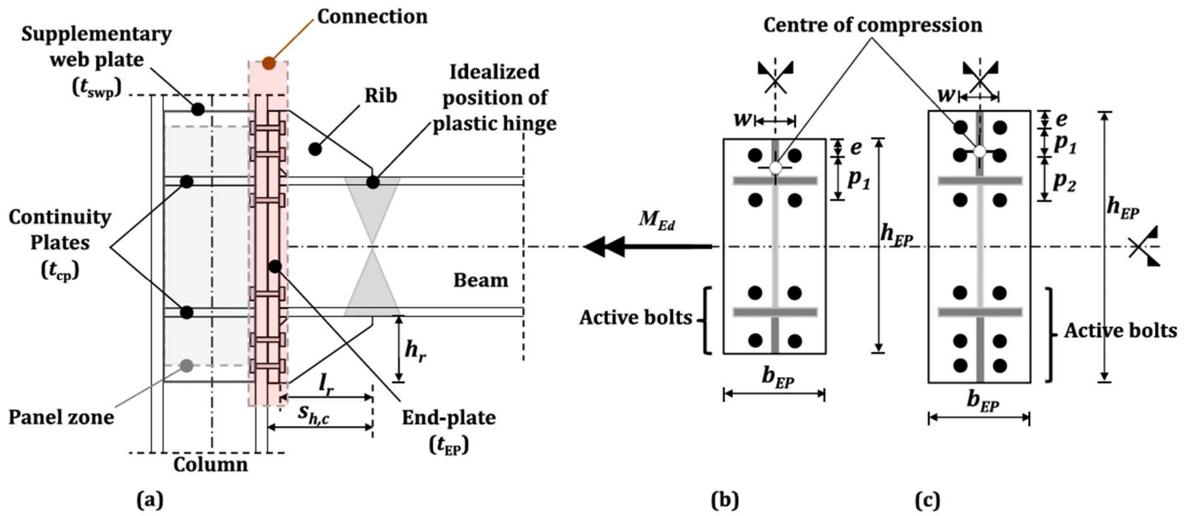

Fig. 1. Geometrical features of the studied ESEP joints.

Although schematizing the joint by means of three macro-components implies disregarding the mutual interactions between the connection and the column nodal area and does not rigorously comply with the philosophy of the component method, such simplified assumption in combination with specific details and geometrical limitations allows easily controlling the expected performance of the joint and the corresponding dissipation mechanism [5-7,29,30]. In the case of ESEP joints, two alternative types of dissipation mechanisms have been promoted, namely either (i) plastic deformations solely in the connected beam or (ii) plastic deformations in both the beam and the connection. In the first case, the joints can be classified as "full strength" with a "non-yielding" connection, while in the second case as "equal strength" joints with a "balanced yielding" connection. This second type of joint may fall in the range of partial strength joints of EN1993-1-8 [1] if the bending resistance of the connection is slightly smaller than the actual plastic bending resistance of the connected beam, but the damage pattern is controlled in order to avoid the contribution of the column panel zone and to enforce the yielding of the beam. In this regard, the connection should not be stronger than the expected ultimate resistance of the beam in order to allow its yielding and distributing the damage between the beam and the connection. As shown in [5-8,29,30], sharing the damage between the beam and the connection aims at reducing the constructional costs and limiting damage concentration in the beam which can be beneficial to repair the building in the aftermath of the severe earthquakes as well as to reduce the demand on the column since both flexural and twisting moments transferred by the beam plastic hinge reduce if the beam damage decreases [5-8].

Therefore, differently from EN 1993-1-8 [1], the required resistance of the connections is evaluated depending on the type and the localization of the plastic mechanism also accounting for the random material variability and strain hardening of the dissipative zone (i.e., either the beam or the connection) as follows:

$$M_{con,Rd} \geq \gamma_{rm} \bullet \gamma_{sh} \bullet \left(M_{b,pl,k} + s_{h,c} \bullet V_{Ed,M}\right) + s_{h,c} \bullet V_{Ed,G} \text{ for full strength connections} \quad (1)$$

$$\left(M_{\mathrm{b,pl,k}} + s_{\mathrm{h,c}} V_{\mathrm{Ed,M}}\right) + s_{\mathrm{h,c}} V_{\mathrm{Ed,G}} \leq M_{con,Rd} < \gamma_{rm} \bullet \gamma_{sh} \bullet \left(M_{\mathrm{b,pl,k}} + s_{\mathrm{h,c}} V_{\mathrm{Ed,M}}\right) + s_{\mathrm{h,c}} V_{\mathrm{Ed,G}} \text{ for equal strength connections} \quad (2)$$

where:

$M_{con,Rd}$ is the design resistance of the connection;
$M_{b,pl,k}$ is the nominal plastic moment of the beam framing the joint, namely evaluated considering the nominal value of the yield stress f_y of steel;
$V_{Ed,M}$ is the shear force due to the formation of plastic hinges with nominal plastic resistance at both beam ends (i.e., $V_{Ed,M}$ = 2 $M_{b,pljk}$ /L_h, L_h being the distance between the plastic hinges at both beam ends);
$V_{Ed,G}$ is the design value of the shear force due to the non-seismic actions;

$s_{h,c}$ is the distance between the centre of the expected plastic hinge (i. e., the section at the tip of the rib stiffener for ESEP joints) and the connection (i.e., the column face), see Fig. 1;
γ_{rm} is the randomness material factor (which was assumed equal to 1.25 in this study, in accordance with [4]);
γ_{sh} is the hardening factor of the plastic hinge (which was assumed equal to 1.2 in this study, in accordance with [29-30]).

It is also worth noting that in this study, the values of both γ_{rm} and γsh have been individually adopted on the basis of the results of former research projects [4,29]. These factors are solely identified as sources of overstrength and the adopted values are not recommended because a comprehensive statistical study would be necessary.

Both Full and Equal strength ESEP joints are intended for applications in MRFs and Dual braced frames, depending on the level of design ductility class, namely: the first is suitable for all ductility classes, and the second ones solely for low-to-moderate ductility classes [29]. It is also worth noting that the design criteria summarized in this section have been partially implemented in the prEN1998-1-2:2022 [31] which is the latest draft of the amended version of EN1998 at the time of drafting the present article.

Fig. 1b, and c show the layout of the tested bolted connections, namely four bolt rows (i.e., one row in the extended part of the end-plate and another one inside the beam profile) and six bolt rows (i.e., two rows in the extended part of the end-plate and on inside the beam profile).

2.2. ADOPTED DETAIL

Fig. 2a shows the shape and the considered details (both welds and geometry) of the tested rib stiffeners. As it can be also observed, the adopted ribs are more compact and shorter (i.e., slope equal to 40°) than those recommended by AISC358 (where a slope equal to 30° is prescribed). This choice derives from background studies [5-8,29,30] that highlighted the feasibility of using shorted rib, thus leading to smaller consumption of welding consumables as well as lower design moment in the

Published in : Engineering Structures (2023), 116386
DOI: 10.1016/j.engstruct.2023.116386
Status : Postprint (Author's version)

connection (the distance $_{Sh,c}$ from the beam plastic hinge to the column face being smaller). Full penetration welds with a chamfer slope equal to 60° have been considered for rib-to-beam and rib-to-end-plate details. In accordance with AISC358 [20], the thickness of the rib was designed as the maximum between the values given by the following conditions:

$$t_{w,r} \geq t_{w,b} \bullet \left(\frac{f_{y,b}}{f_{y,r}} \right) \tag{3}$$

$$\frac{h_r}{t_{w,r}} \leq 0,56 \sqrt{\frac{E}{f_{y,r}}} \tag{4}$$

where $t_{w,r}$ is the thickness of the rib web; $t_{w,b}$ is the thickness of the beam web; $f_{y,r}$ is the yield strength of the rib web; $f_{y,b}$ is the yield strength of the beam; h_r is the depth of the rib web; E is the elastic modulus of the steel.

For that concerns the evaluation of the design resistance of the end-plate connection as a "macro-component" of both full and equal strength joints, solely the bolt rows outer from and the internal one close to the beam flange in tension have been considered [5-8,29,30], thus considering three and two active bolt rows in tension in the six and four bolt rows configurations, respectively, which imply having only a single active bolt row within the beam flange in tension and the axis of the beam. In addition, there are some components that have been intentionally kept out from the analytical model of the connection resistance such as the beam web and the beam flange in compression (although envisaged by EN1993-1-8 [1]) because they are parts of the beam plastic hinge that is intentionally enforced. In addition, the column web in transverse tension and compression components have not been accounted for in the calculation of the resistance since supplementary stiffening plates onto the column web have been used as detailed in Fig. 2. All these assumptions lead to simplistically estimating the moment resistance of the bolted connections considering solely the contribution of the end-plate in bending and column flange in bending independently from the shear resistance of the column web panel. In order to avoid a premature yielding of the "bolts in tension" and so, to enhance the ductility of the end-plate connection of equal strength bolted connections, the end-plate thickness tp was also designed to comply with the following criterion based on [29,30]:

$$t_p \leq 0,30 \bullet d \bullet \sqrt{\frac{f_{u,b}}{f_{y,p}}} \tag{5}$$

where d is the nominal diameter of the bolt; $f_{u,b}$ is the ultimate tensile strength of the bolt; $f_{u,b}$ is the tensile yield strength of the material of the end-plate.

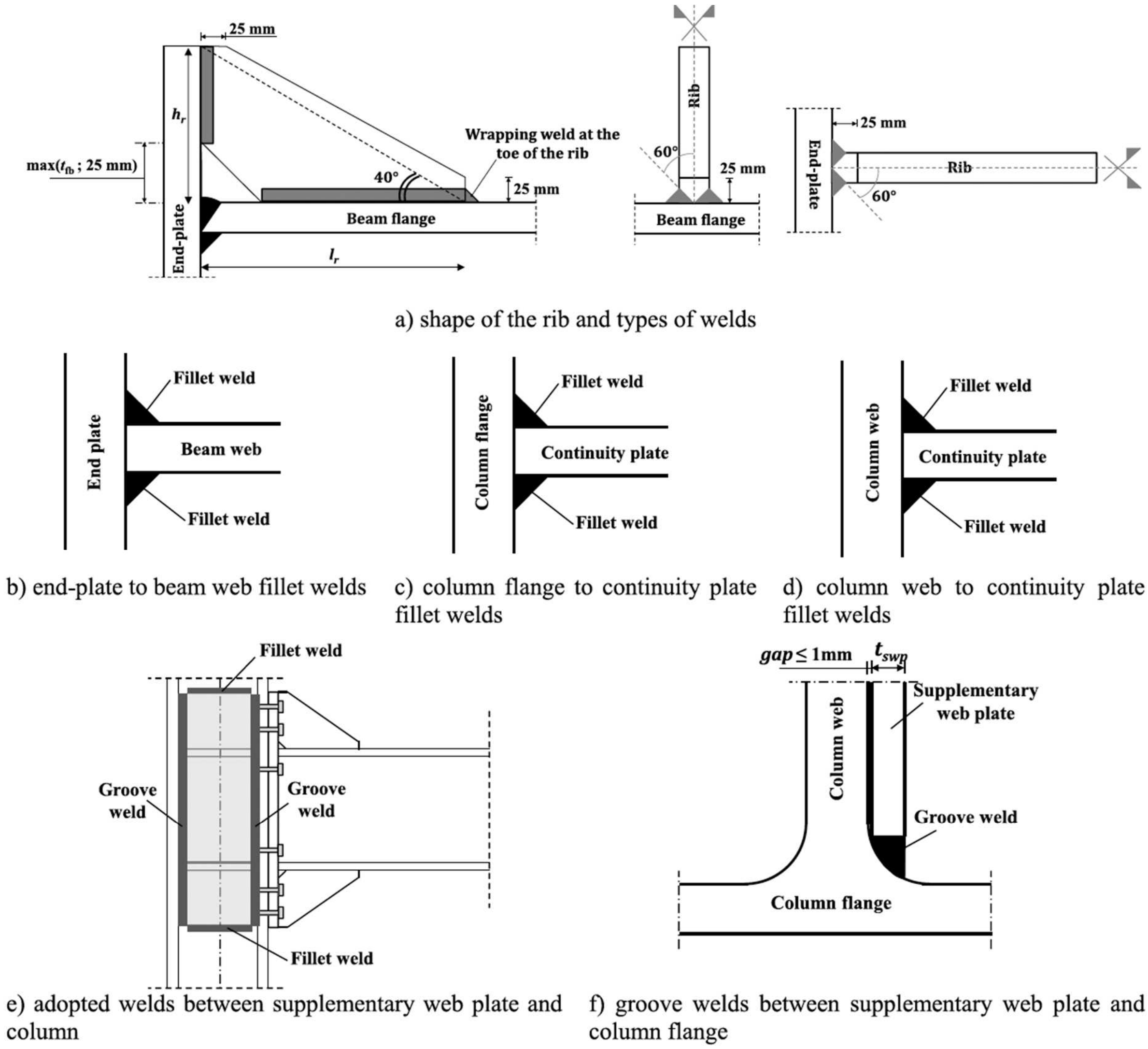

Fig. 2. Main details of the tested ESEP joints.

To calculate the moment resistance, the lever arm of each bolt row was evaluated assuming that the centre of compression is in the centroid of the beam flange and rib web in accordance with [7,8,12].

The shear resistance of the column web panel $V_{wp,Rd}$ was calculated in accordance with EN1993-1-8 without the additional resistance of continuity plates and verified to be greater than the minimum resistance of either the beam (from Eq. (1)) or the connection (from Eq. (2)). Supplementary web plates were used to strengthen the nodal zone as detailed in Fig. 2e,f in the cases where the alone column web was not sufficient to guarantee the required shear resistance. In these cases, the resisting shear area A_v has been assumed as the sum of column shear area $A_{v,c}$ and the entire gross area of the additional web plates $A_{v,p}$, without limiting the second contribution to the thickness of the column web panel even if such a limitation is recommended in EN1993-1-8 [1]. The stability of the supplementary plates was verified in accordance with be EN 1993-1-8 [1]. The depth of the supplementary web plates was set equal to the depth of the end-plate, which was greater than the effective width of the column web in tension and compression.

Published in : Engineering Structures (2023), 116386
DOI: 10.1016/j.engstruct.2023.116386
Status : Postprint (Author's version)

Continuity plates were used to restrain the column flange and their thickness was assumed equal to the rounded up value of the thickness of the beam flange. The corner clip of the continuity plate was detailed to avoid interference with the fillet radius of hot-rolled columns (i.e., the fillet radius +1 mm).

The bolts of the studied connections were tightened with the torque method in accordance with EN1090-2 [33] applying the preload force given by EN1993-1-8 [1].

The types of welds between the different joint components are given in Fig. 2. MAG welds with G 46 welding wires in accordance with ISO 14341-A [32] (i.e., f_y > 460 MPa and toughness greater than 47 J at -40 °C) were used in all tested joints.

All specimens were manufactured in accordance with the requirements for execution class 3 (EXC3) given in EN1090-2 [33]. The quality of all welds was controlled by means of magnetoscopic tests, and additional ultrasonic spot-checks were carried out on about 25% of these welds.

3. Acceptance criteria

The seismic performance of the tested joints was verified against two different acceptance criteria, namely according to EN1998 [2. 31] (see Fig. 3a) and AISC341 [19] (see Fig. 3b). In the first case, the seismic performance of the joint is deemed satisfactory if the provided plastic rotation " θ_p" (which is defined as in Fig. 3a and evaluated without the elastic contribution " θ_y" of beam and column) is greater than 0.03 rad for highly ductile structures (i.e., DCH concept in EN1998-1:2005 [2] and DC3 concept in prEN1998-1-2:2022 [31]) or 0.02 rad for moderate ductile structures (i.e., DCM in EN1998-1:2005 [2] and DC2 concept in prEN1998-1-2:2022 [31]).

The AISC341 [19] criterion requires that the joint should withstand a moment not smaller than 80% of the plastic flexural resistance of the beam at a story drift angle " $\theta_{0.8Mp}$" equal to 0.04 rad for highly ductile structures (i.e., special moment frames in AISC341 [19]) or 0.02 rad for moderate ductile structures (i.e., intermediate moment frames in AISC341 [19]).

In both cases, the specimen is considered qualified if the test succeeds at least one full cycle with the minimum requested rotation/storey drift in accordance with the first-cycle response envelopes depicted in Fig. 3.

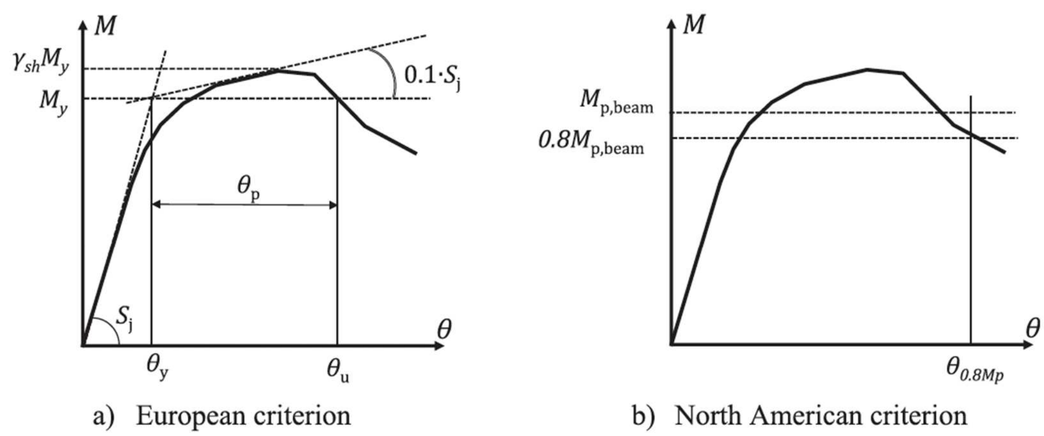

Fig. 3. Acceptance criteria of the seismic performance of the tested joints.

Published in : Engineering Structures (2023), 116386
DOI: 10.1016/j.engstruct.2023.116386
Status : Postprint (Author's version)

4. Experimental tests

4.1. EXPERIMENTAL PROGRAM

The types of tested full and equal strength joints and their relevant features are summarized in Table 1. The specimens are identified by means of the following labelling code:

ES (Extended Stiffened) 1/2/3 (for joints with shallow/intermediate/deep members, respectively) - TS (T-Shape, namely external joints) - E/Esp/F (Equal strength / Equal strength with shot peening / Full strength) - C1/C2/CA/M (loading protocol, see Table 1).

As it can be observed, three groups of full strength joints and three others of equal strength joints have been tested. Each group was representative of a different beam/column assembly to investigate the influence of shallow, intermediate, and deep profiles on the seismic performance of the considered joints. All specimens were made of S355 steel grade, and the column web panel was strengthened as shown in Fig. 2 to resist almost elastically. High strength preloaded 10.9 HV bolts with K2 class were used for all studied connections. In addition, three equal strength joints were manufactured using shot peening (see the specimens identified with the sub-code "Esp" in Table 1) for the end- plate-to-rib and end-plate-to-beam welds to investigate the potential beneficial effect of such treatments on the ductility of equal strength connections that should develop plastic deformations. At least, two cyclic tests have been performed per type of configuration by imposing the AISC341 protocol [19] (see in Table 1 the specimens with sub-ID "C1" and "C2" that refer to the first and the second test using the AISC341 protocol for two nominally identical specimens). Additionally, as indicated by the sub-ID "M" in Table 1, two monotonic tests have been performed on a couple of full strength joints (i.e., one with the shallower and another with the deeper profiles) in order to investigate the influence of the beam-to-column ratio on the monotonic resistance and rigidity of these joints. It is also worth noting that one cyclic test was carried out by applying an alternative loading protocol that was developed within the EQUALJOINTS project [29] (see in Table 1 the specimen with sub-ID "CA").

In Table 1 the geometrical features of the end-plate are given in terms of depth (h_{EP}), width (b_{EP}) and thickness (t_{EP}). The bolt diameter (d), the vertical distance from the edge of the outermost bolt row (e), the horizontal distance between bolts (w), the spacing between the first and the second active bolt rows (p1), and the distance between the second and the third active bolt rows (p_2) are also reported for the bolted details (where the definition of active bolt rows is shown in Fig. 1). In addition, the thickness of the continuity plates (t_{CP}) and the configuration of supplementary column web plates and their thickness (t_{SWP}) are given. Moreover, both the design demand (M_{con},E_d) and the resistance ($M_{con,Rd}$) of each joint (which have been evaluated considering the design strength of the materials) are reported.

Published in : Engineering Structures (2023), 116386
DOI: 10.1016/j.engstruct.2023.116386
Status : Postprint (Author's version)

Table 1
Geometrical and mechanical features of the tested joints.

Specimen ID	Loading Protocol	Design Demand $M_{con,Ed}$ (kNm)	Design Resistance $M_{con,Rd}$ (kNm)	$s_{h,c}$	End-Plate			Bolts (rows, diameter, and spacing)						Continuity Plates	Supplementary column web plates	
				(mm)	h_{EP} (mm)	b_{EP} (mm)	t_{EP} (mm)	Bolt rows -	d (mm)	e (mm)	w (mm)	p_1 (mm)	p_2 (mm)	t_{CP} (mm)	Side -	t_{SWP} (mm)
ES1-TS-E-C1	AISC341 [19]	380.2	390.3	158	600	280	18	4	27	50	160	160	–	14	single	8
ES1-TS-E-C2	AISC341 [19]				600	280	18		27	50	160	160	–	14	single	8
ES1-TS-Esp-C	AISC341 [19]				600	280	18		27	50	160	160	–	14	single	8
ES1-TS-F-C1	AISC341 [19]	589.7	592.3	260	760	260	25	6	30	50	150	75	160	14	double	8
ES1-TS-F-C2	AISC341 [19]				760	260	25		30	50	150	75	160	14	double	8
ES1-TS-F-M	Monotonic				760	260	25		30	50	150	75	160	14	double	8
ES2-TS-E-C1	AISC341 [19]	645.7	645.5	210	770	300	20	4	30	55	160	200	–	15	single	8
ES2-TS-E-C2	AISC341 [19]				770	300	20		30	55	160	200	–	15	single	8
ES2-TS-Esp-C	AISC341 [19]				770	300	20		30	55	160	200	–	15	single	8
ES2-TS-F-C1	AISC341 [19]	990.7	992.7	275	870	280	25	6	30	50	150	75	180	15	double	10
ES2-TS-F-C2	AISC341 [19]				870	280	25		30	50	150	75	180	15	double	10
ES2-TS-F-CA	Alternative [29]				870	280	25		30	50	150	75	180	15	double	10
ES3-TS-E-C1	AISC341 [19]	1386	1388	317	1100	300	22	6	36	55	160	95	210	20	single	15
ES3-TS-E-C2	AISC341 [19]				1100	300	22		36	55	160	95	210	20	single	15
ES3-TS-Esp-C	AISC341 [19]				1100	300	22		36	55	160	95	210	20	single	15
ES3-TS-F-C1	AISC341 [19]	2085	2087	325	1100	280	30	6	36	55	160	95	210	20	double	15
ES3-TS-F-C2	AISC341 [19]				1100	280	30		36	55	160	95	210	20	double	15
ES3-TS-F-M	Monotonic				1100	280	30		36	55	160	95	210	20	double	15

ES1 assembly: Beam IPE360 – Column HEB280.
ES2 assembly: Beam IPE450 – Column HEB340.
ES3 assembly: Beam IPE600 – Column HEB500.

4.2. EXPERIMENTAL SETUP AND TESTING PROCEDURE

The tests have been carried out in two different laboratories. Twelve specimens corresponding to the groups of ES1 and ES2 configurations were tested at the University of Naples Federico II (hereinafter also referred to as "UNINA"), while 6 specimens corresponding to ES3 configurations were tested at the University of Liege (hereinafter also referred to as "ULiege"). Therefore, two experimental setups have been adopted due to the different facilities of the involved laboratories, see Fig. 4. In both cases, the specimens were tested horizontally with displacement history applied at the tip of the beam, while the columns were restrained at one end by a pinned restraint and a slider restraint at the opposite end in order to simulate the beam-column sub-assembly extracted from the contraflexure points of a moment frame under lateral forces. The axial force was not applied to the columns of the tested specimens because this parameter does not affect the response of full strength panel zone in the range of interest for EC8-compliant ductile MRFs (i.e., not exceeding 0.3 times the plastic axial resistance of the column) as widely proved by the experimental and numerical studies carried out in the research project HSS-SERF [34] and also verified numerically in research project EQUALJOINTS [29].

Displacement transducers have been used to record the deformations of the specimens during the tests as shown in Fig. 4. The monitored global parameters were the interstorey drift angle $\theta = \delta/L$ (being δ the displacement at the beam tip and L the length from the column axis to the beam tip) and bending moment M at the column axis and these data are available in Annex of the present article.

Strain gauges were also used to evaluate the local response of the joints, and displacement transducers were applied to measure the rotations of the column panel zone and the end-plate connection. In particular, the panel zone rotation (θ_{wp}) is given by transducers diagonally fixed on the column web panel at the level of continuity plates, as follows:

$$\theta_{wp} = (\Delta_1 + \Delta_2) \bullet \frac{\sqrt{a^2 + b^2}}{2ab} \qquad (6)$$

where a and b are the horizontal and vertical distances between the measuring points; Δ 1 and Δ 2 are the displacements recorded by transducers diagonally fixed on the column web panel.

The rotation of the connection (θ_{con}) is evaluated as the total joint rotation (θ_J) without the contribution (θ_{wp}) of the column panel zone, namely as follows:

Published in : Engineering Structures (2023), 116386
DOI: 10.1016/j.engstruct.2023.116386
Status : Postprint (Author's version)

$$\theta_{con} = \theta_J - \theta_{wp} = \frac{(\delta_1 - \delta_2)}{d_t} - (\Delta_1 + \Delta_2) \bullet \frac{\sqrt{a^2 + b^2}}{2ab} \qquad (7)$$

where δ_1 and δ_2 are the displacements recorded by transducers 7 and 8 (see Fig. 4) and d_t is the distance between these transducers.
As anticipated in section 4.1, both monotonic and cyclic loading protocols were used. The AISC341-16 loading protocol was used to qualify the seismic performance of the joints, while an alternative loading protocol specifically developed in the RFCS EQUALJOINTS project [29] (hereinafter also referred to as "EJ" protocol) was also used for the sake of comparison. In fact, this alternative loading protocol is slightly less demanding than the one recommended by AISC341 [19] as it can be recognized from Fig. 5, which shows the history of interstorey drift angle imposed by AISC341 [19] and EJ [29] protocols, as well as the comparison of their corresponding cumulative demand functions CDF that give the relation between the imposed interstorey drift angle per cycle (θ_i) normalized to 0.04 rad, namely $|\theta_i|/0.04$.

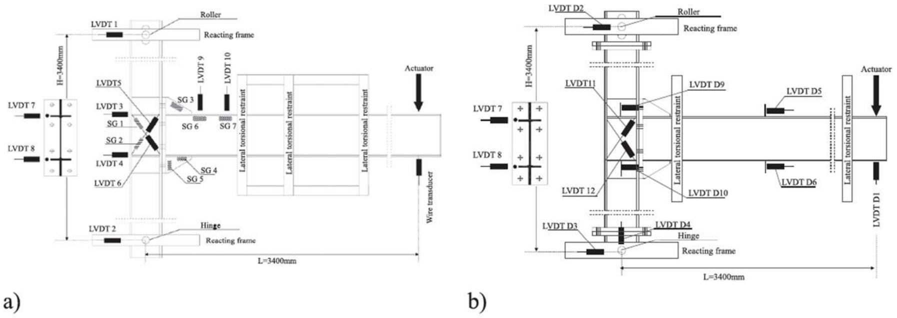

Fig. 4. Experimental setup at UNINA (a) and ULiege (b).

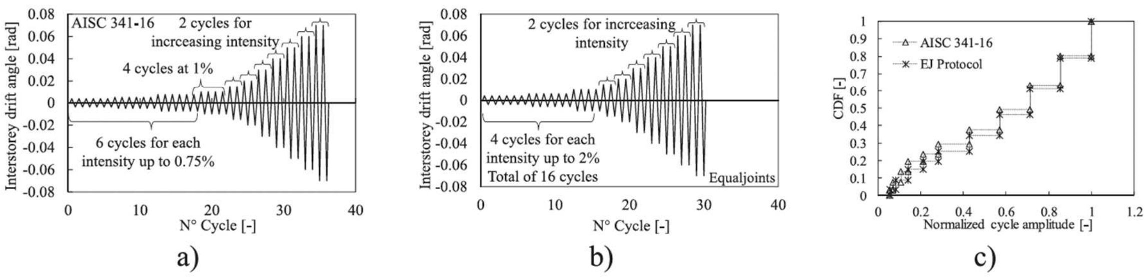

Fig. 5. Adopted loading protocols for cyclic tests: AISC341 (a), alternative protocol (b), comparison of cumulative demand functions (c).

The specimens tested at UNINA were subjected to increasing rotations up to the maximum stroke of the actuator (which corresponded to slightly less than 7% of interstorey drift angle). Once reached such a level of deformation, the tests were conducted at constant amplitude till the full fracture of the specimens. The tests at ULiege were terminated once reached the rotation of interest with a unique exception (i.e., specimen ES3-TS-F-C2) which was prematurely terminated due to technical problems with the testing setup.

4.3. MATERIAL PROPERTIES

All members and plates were made of S355 steel grade and preloaded HR 10.9 bolts were used (see Section 2). A total number of 66 material coupon tests were carried out at UNINA and ULiege to characterize the stress-strain behaviour of the materials; the mean values of their main mechanical parameters are reported in Table 2.

Table 2
Mean values of the main mechanical parameters of the tested materials.

Elements (profiles/plates/ bolts)	Sampled location/ type	Elastic modulus (N/mm^2)	$f_y/f_{y,nom}$ (-)	Yield stress (f_y) (N/mm^2)	Ultimate stress (f_u) (N/mm^2)	Elongation (%)
IPE 600	Web	207,135	1.30	461.9	506.2	33.0
	Flange	184,153	1.34	475.8	552.2	35.5
IPE 450	Web	204,118	1.20	425.6	516.2	30.7
	Flange	206,095	1.16	410.9	517.1	32.9
IPE 360	Web	205,626	1.11	395.7	511.0	32.1
	Flange	195,124	1.07	381.2	518.2	30.3
HEB 280	Web	208,199	1.08	383.6	497.5	27.0
	Flange	203,616	1.09	387.0	502.8	31.1
HEB 340	Web	207,850	1.18	420.2	497.7	32.0
	Flange	217,136	1.37	486.2	565.8	29.5
HEB 500	Web	212,481	1.23	436.2	501.0	34.6
	Flange	222,699	1.23	435.1	552.4	34.7
Plates	t_{ep} = 15 mm	203,220	1.29	459.2	567.3	33.8
	t_{ep} = 18 mm	211,573	1.18	417.9	551.7	33.4
	t_{ep} = 20 mm	209,002	1.43	509.3	563.4	20.6
	t_{ep} = 25 mm	196,203	1.30	459.8	589.8	32.9
	t_{ep} = 30 mm	211,254	0.97	344.5	485.6	41.3
Bolts	d = 27 mm	211,700	1.05	944.2	1172.7	2.6
	d = 30 mm	204,100	1.12	1009.4	1254.1	2.1

5. Experimental results

Fig. 6 summarizes the experimental response curves of all tested joints in terms of the moment at the column centreline vs. interstorey drift angle. As it can be observed, the overall response of all tested joints is characterized by rounded and stable hysteretic loops without appreciable degradation up to 0.04 rad. In the case of full strength joints, the degradation of the resistance is due to the activation of local buckling phenomena in the beam plastic hinge. Resistance degradation is less pronounced in equal strength joints and pinching is also negligible, notwithstanding the yielding of the end-plate and the relevant gap opening that was observed in all tested equal strength joints. Comparing the response of the tested beam-column assemblies, it can be observed that the degradation of the cyclic response of ES3 set (i.e., the specimens having the deeper beam) occurs for capping rotations smaller than those experienced by ES1 and ES2 joints. However, all tested joints exceeded an interstorey drift angle of 0.04 rad.

The comparison between the hysteretic responses of ES3-TS-F specimens (see Fig. 6) shows that the differences between tests using the AISC 341 [19] and the alternative EJ protocol [29] are negligible. This result is mainly due to the fact that the EJ protocol has merely fewer elastic cycles than the AISC341 protocol.

Published in : Engineering Structures (2023), 116386
DOI: 10.1016/j.engstruct.2023.116386
Status : Postprint (Author's version)

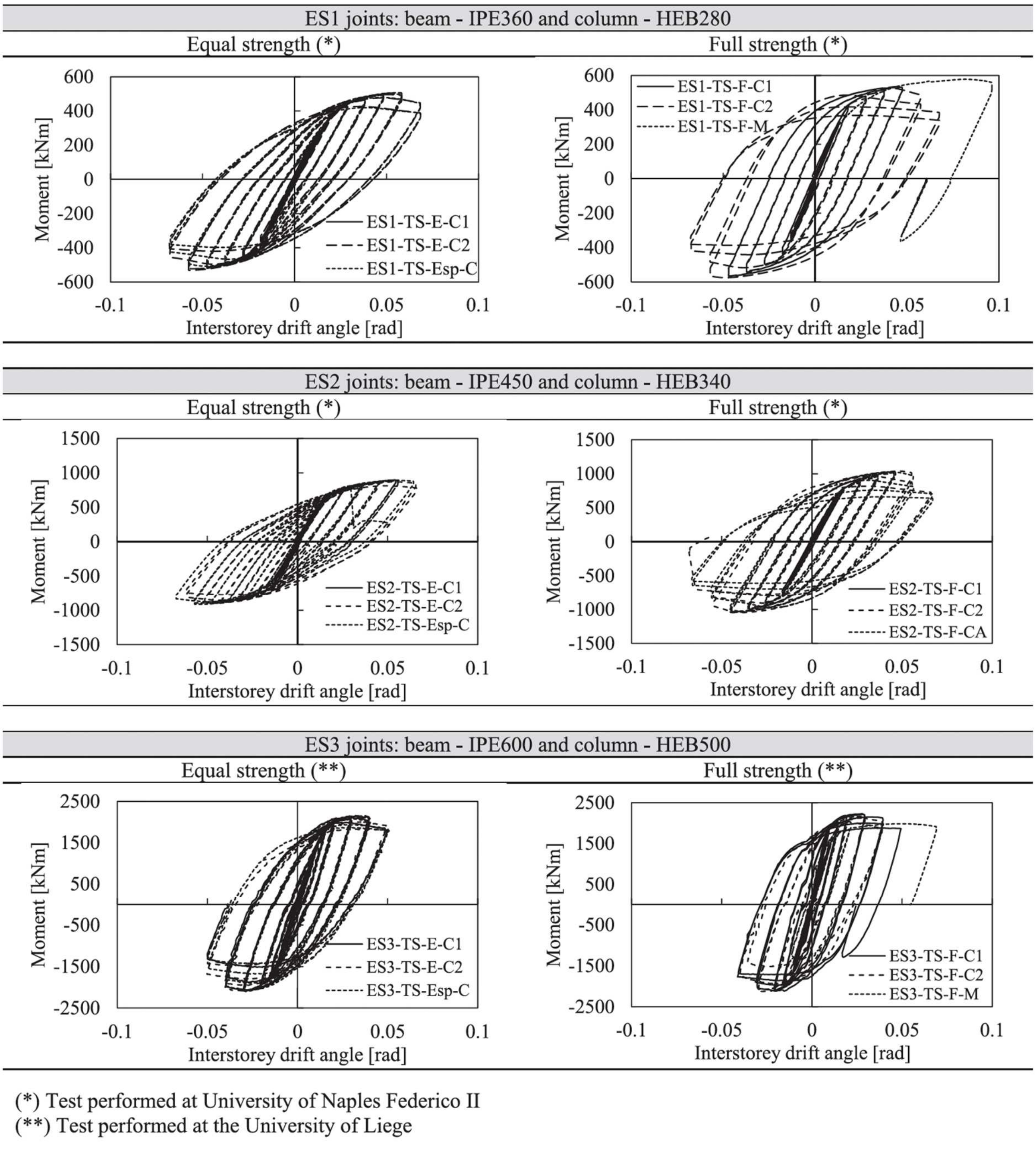

Fig. 6. Experimental moment-interstorey drift angle response curves.

The comparison of the hysteretic curves of equal strength joints with and without shot peening (i.e. those identified with the subscript "sp") for the welds of the connection clearly show that this treatment does not give any beneficial effect on the ductility of the joints since the response curves are well overlapped and the damage patterns (see Figs. 7 and 8) are the same. Therefore, it can be concluded that there is no actual need to adopt such treatment.

Fig. 7 summarizes the overall views of the failure modes exhibited by the tested joints, while the patterns of cracks in the damaged specimen are given in Fig. 8 at the end of the tests. Consistently with their response curves, the full strength joints exhibited the formation of the plastic hinge in the beam

Published in : Engineering Structures (2023), 116386
DOI: 10.1016/j.engstruct.2023.116386
Status : Postprint (Author's version)

at the tip of the rib stiffener with progressive deterioration due to local buckling and fracture of the beam flange due to low-cycle fatigue at the end of the imposed constant amplitude cycles (see Table 3 where the number of constant amplitude cycles per specimen is reported).

Published in : Engineering Structures (2023), 116386
DOI: 10.1016/j.engstruct.2023.116386
Status : Postprint (Author's version)

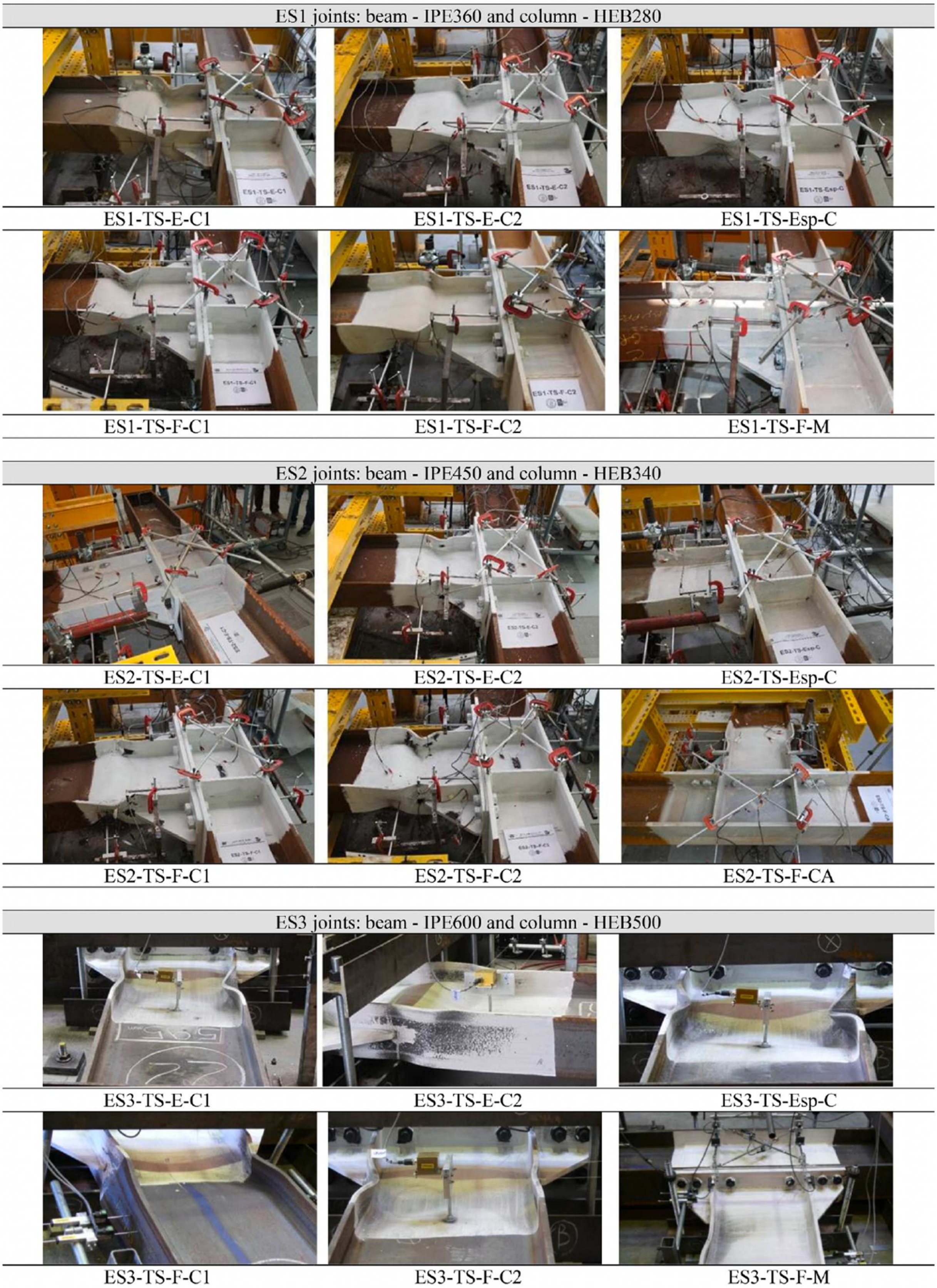

Fig. 7. Failure modes of the tested joints at the first cycle imposed by the maximum stroke of the actuator.

Published in : Engineering Structures (2023), 116386
DOI: 10.1016/j.engstruct.2023.116386
Status : Postprint (Author's version)

Fig. 8. Pattern of cracks in the damaged joints at the end of the tests (i.e., for ES1 and ES2 after the constant amplitude cycles at the maximum stroke of the actuator).

Table 3
Cumulated imposed interstorey drift angle and ductility.

Assembly	Number of cycles at constant amplitude (max stroke of the actuator)	CIDA	θ_y	CID	
				θ = 4%*	end of the test
	[-]	[rad]	[rad]	[-]	[-]
ES1-TS-E-C1	10	4.19	0.019	74	222
ES1-TS-E-C2	10	4.19	0.018	77	232
ES1-TS-Esp-C	9	3.95	0.021	67	191
ES1-TS-F-C1	5	2.99	0.016	87	187
ES1-TS-F-C2	8	3.71	0.016	89	238
ES2-TS-E-C1	2	2.27	0.016	86	140
ES2-TS-E-C2	4	2.75	0.016	86	171
ES2-TS-Esp-C	2	2.27	0.015	91	149
ES2-TS-F-C1	2	2.27	0.015	94	154
ES2-TS-F-C2	3	2.51	0.016	86	155
ES2-TS-F-CA	3	2.51	0.016	86	155
ES3-TS-E-C1	–	1.39	0.013	104	104
ES3-TS-E-C2	–	1.39	0.014	101	101
ES3-TS-Esp-C	–	1.39	0.014	99	99
ES3-TS-F-C1	–	1.49	0.009	158	170
ES3-TS-F-C2	–	1.39	0.011	129	129

The equal strength joints showed plastic deformations in both the beam (i.e., local buckling of the flanges) and the connection (i.e. end- plate in bending), thus confirming the expected behaviour and the effectiveness of the design assumptions. It should be highlighted that ES2-E and ES3-E specimens showed the opening of a crack from the flange to the web of the beam and the formation of the cracks anticipated in the case of deeper beams (i.e., at about 0.03 rad for ES3-E and 0.06 rad for ES2-E). In both ES2-E and ES3-E, the cracks in the beams initiated from the toe of the weld at the rib tip and propagated into the beam web, see Fig. 8. In addition, some signs of crack formation were also observed in the outermost parts of the welds connecting the rib stiffener and the end-plate. It is also worth noting that the patterns of the cracks in Fig. 8 correspond to those at the end of the tests where constant amplitude cycles were applied to ES1 and ES2 specimens once reached the maximum stroke of the actuator (see Table 3). In this case, the ES1- TS-E-C1 specimen and both full and equal strength ES2 with the unique exception of ES2-TS-F-CA exhibited the flange and half the depth of the web of the deep beam fracture that initiated outside the wrapping weld at the toe of the rib stiffener. It can be argued that such location of the crack is an area where both localization of stresses (i.e., the tensile stress in the rib in combination with the longitudinal tensile stress in the beam flange) are expected and the heat affected zone (HAZ) may reduce low- cycle fatigue resilience and ductility.

All other ES1 specimens and the ES2-TS-F-CA showed the cracking of the beam flange in the mid-length of the plastic hinge due to the cumulation of damage in the bent beam flange due to its local plastic buckling, which is the typical expected response of a plastic hinge in a ductile steel beam. However, it should be noted that the seismic response of all joints was satisfactory since the beam fracture occurred at a rotation demand greater than the required threshold. The cumulated imposed interstorey drift angle

$$CIDA = \sum_i \theta_i$$

and the cumulated imposed ductility

$$CID = \sum_j \left|\theta_{j,max} - \theta_{j,min}\right| / \theta_y$$

are reported in Table 3, where θ_i is the interstorey drift angle at i-th cycle, $\theta_{j,max}$ and $\theta_{j,min}$ are the maximum and minimum rotation at the j-th cycle, and θ_y is the yield interstorey drift angle. The obtained values of CIDA and CID are substantially greater than those experienced by welded joints with European profiles [35,36] and in line with those numerically estimated by [37]. In addition, both ES1 and ES2 exhibited a ductility greater than those shown in [17,25].

Figs. 9 and 10 show the moment vs. rotation curves of the connection, the column web panel and the interstorey drift angle, the latter for the sake of comparison, for full and equal strength joints (one specimen per type is reported since the behaviour is similar for those of the same assembly). The contribution of joint components differs for full strength and equal strength joints. In the former case, the rotation of the beam plastic hinge is the main contribution to the interstorey drift angle, the rotation of the connection and distortion of column web panel that behave in elastic range being negligible, see Fig. 9b,c,e,f,h,i.

Equal strength end-plate connections exhibited plastic deformationsES1-TS-F-C2 and provided appreciable rotations (from 10 % to 20% of the total rotation) while the column web panel were still in the elastic range. In this regard, it is also worth noting that the rib stiffeners also enlarge the effective height of the panel zone which is beneficial to decrease the shear force demand in the nodal area of the column [7,8], thus resulting in an improved resistance as also shown for haunched connections by [38]. As a general remark, it should be noted that, even for equal strength joints, the plastic rotation of the beam mainly contributed to the overall rotation of the beam-column joints.

Published in : Engineering Structures (2023), 116386
DOI: 10.1016/j.engstruct.2023.116386
Status : Postprint (Author's version)

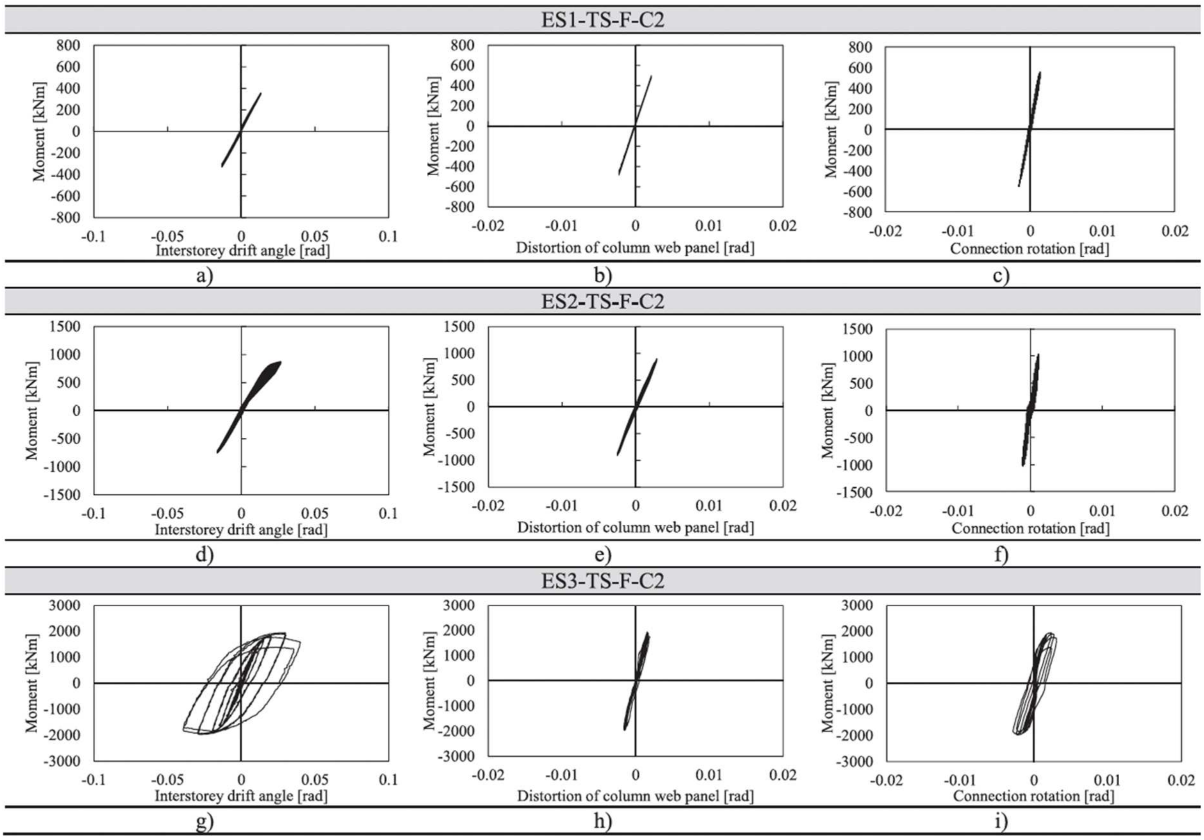

Fig. 9. Moment vs. interstorey drift angle, column web panel and connection rotation of full strength joints.

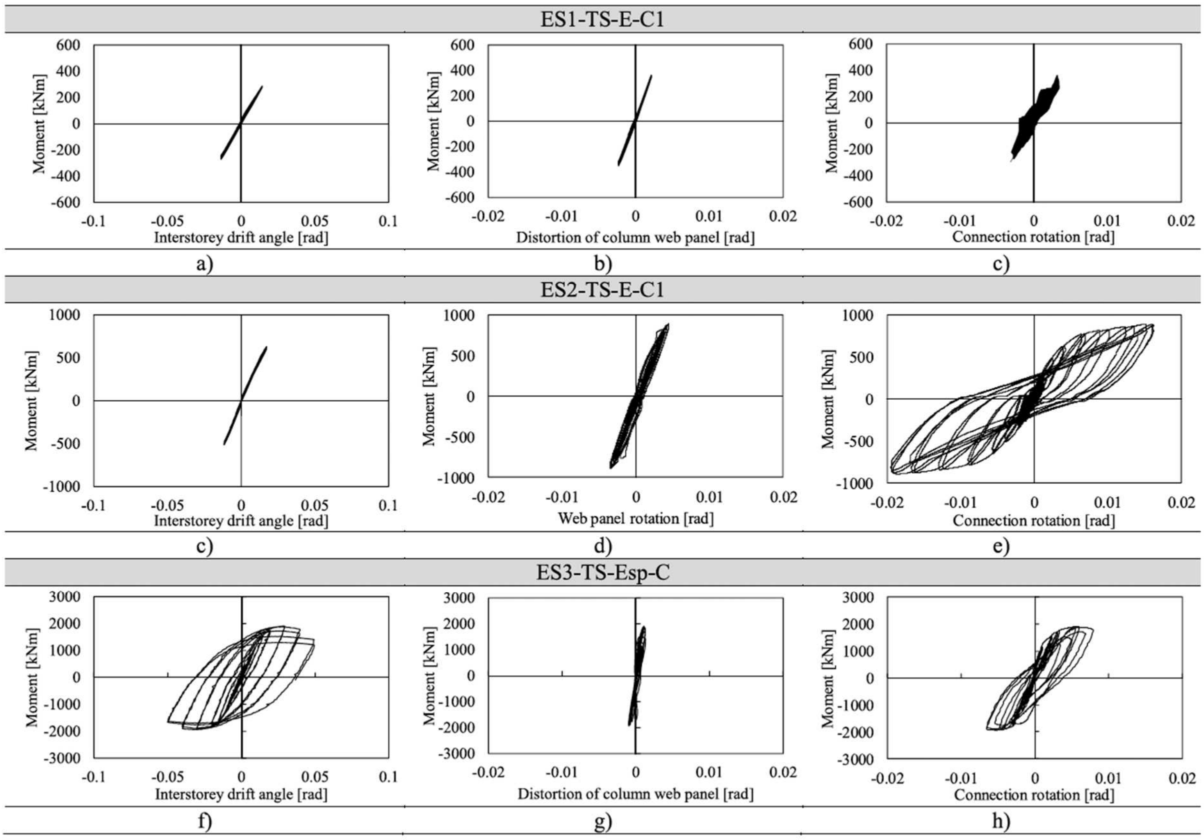

Fig. 10. Moment vs. interstorey drift angle, column web panel and connection rotation of equal strength joints.

Published in : Engineering Structures (2023), 116386
DOI: 10.1016/j.engstruct.2023.116386
Status : Postprint (Author's version)

6. Performance parameters and compliance with pre-qualification limits

The considered performance parameters have been derived as the smaller values measured from both the sagging (+) and hogging (-) backbone of the moment-interstorey drift angle curves of the tested joints and, as described in Fig. 3, are the strain hardening coefficient (γ_h), the yield interstorey drift angle (θ_y), the ultimate interstorey drift angle (θ_u), the plastic rotation (θ_p), and the rotation ($\theta_{0.8Mp}$).

For the sake of example, Fig. 11 summarizes the backbone curves for full and equal strength ES1 joints, while Table 4 reports the measured values of all considered performance parameters. With this regard, it is worth noting that the values of ($\theta_{0.8Mp}$) are the maximum rotations achieved during the test even if the corresponding moments are greater than $0.8M_p$. Therefore, the tested joints may guarantee a greater ductility than the value reported in Table 4. However, all specimens met the EC8 [2,31] and AISC341 [19] prequalification requirements for highly ductile structures, since the "θ_p" and "$\theta_{0.8Mp}$" are greater than 0.03 rad 0.04 rad, respectively with the unique exception of ES3-TS-F- C2, whose test was prematurely terminated due to technical problems with the testing setup. Therefore, both full strength and equal strength extended stiffened end-plate joints can be used in high ductile structures.

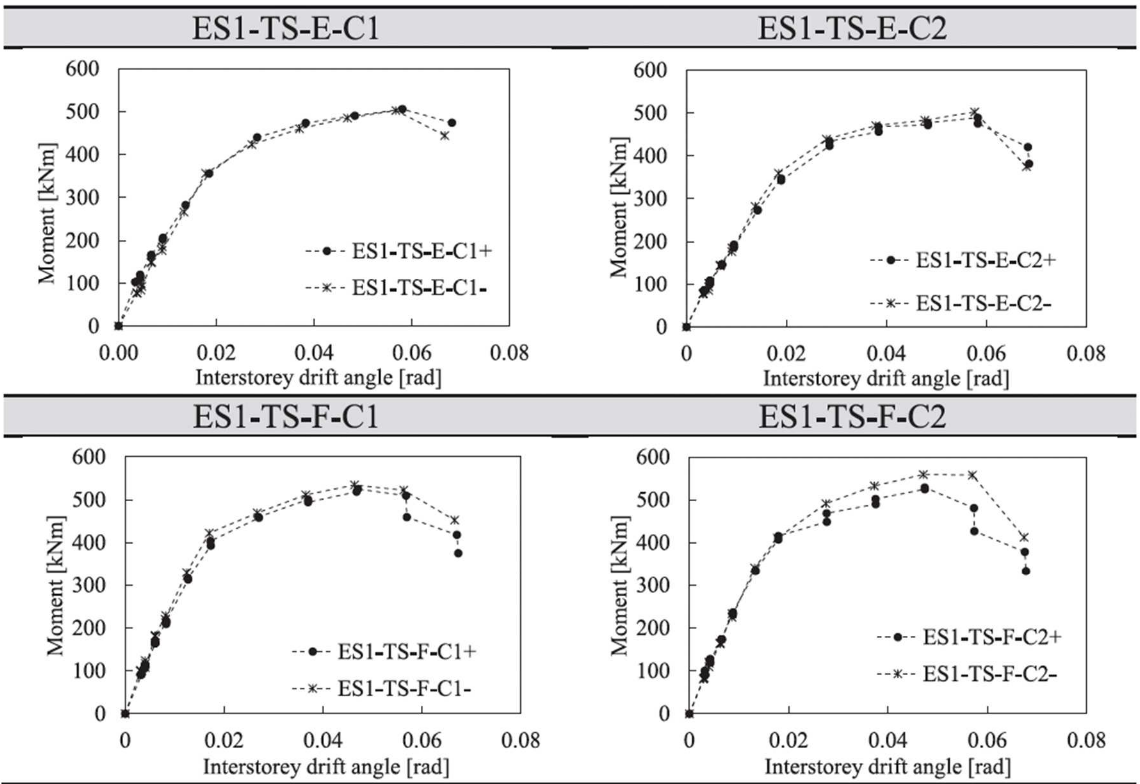

Fig. 11. Sagging (+) and hogging (−) backbone of the moment-interstorey drift angle curves of ES1 joints.

Table 4
Performance parameters of the tested joints.

Specimens	γ_{sh} [-]	θ_y [rad]	θ_u [rad]	θ_p [rad]	$\theta_{0.8Mp}$ [rad]
ES1-TS-E-C1	1.17	0.019	0.068	0.049	0.068 (*)
ES1-TS-E-C2	1.19	0.018	0.068	0.050	0.068 (*)
ES1-TS-Esp-C	1.13	0.021	0.064	0.043	0.069 (*)
ES1-TS-F-C1	1.17	0.016	0.064	0.048	0.067 (*)
ES1-TS-F-C2	1.21	0.016	0.062	0.047	0.068 (*)
ES1-TS-F-M	1.25	0.017	0.094	0.078	0.094 (*)
ES2-TS-E-C1	1.21	0.016	0.063	0.047	0.063 (*)
ES2-TS-E-C2	1.17	0.016	0.066	0.049	0.066 (*)
ES2-TS-Esp-C	1.21	0.015	0.064	0.049	0.064 (*)
ES2-TS-F-C1	1.21	0.015	0.062	0.047	0.065 (*)
ES2-TS-F-C2	1.19	0.016	0.061	0.045	0.066 (*)
ES2-TS-F-CA	1.17	0.016	0.061	0.044	0.067 (*)
ES3-TS-E-C1	1.15	0.013	0.051	0.037	0.051 (*)
ES3-TS-E-C2	1.14	0.014	0.049	0.035	0.049 (*)
ES3-TS-Esp-C	1.10	0.014	0.043	0.036	0.050 (*)
ES3-TS-F-C1	1.20	0.008	0.049	0.042	0.049 (*)
ES3-TS-F-C2	1.15	0.011	0.040	0.029	0.040 (**)
ES3-TS-F-M	1.17	0.010	0.068	0.058	0.068 (*)

(*) Maximum rotation permitted by the testing setup.
(**) Prematurely interrupted due to technical problems with the testing setup.

It can be observed that the strain hardening coefficient is relatively uniform for the same category of joints, namely the mean γ_{sh} is about 1.19 (coefficient of variation equal to 2.5%) for full strength joints, while ysh is about 1.16 (coefficient of variation equal to 3.2%) for equal strength joints. Therefore, considering that the ratio Yrm between the mean value of the yield stress of the beam over the corresponding nominal value is about 1.2 (coefficient of variation equal to 8.4%), the mean overall over-strength factor (γ_{rm} x γ_{sh}) for full strength joints is equal to 1.43, thus confirming that the adopted design value for full strength joints (i.e., 1.25 x 1.2 = 1.5) was effective to guarantee the design objective although a bit conservative. The mean γ_{rm} x γ_{sh} for equal strength joints is equal to 1.40, which is substantially greater than the design resistance of these joints due to the actual strength of the materials (i.e., greater than the design values) as well as the hardening developed by the end-plate in bending of the ESEP connections.

7. Fem analyses

7.1. MODELLING ASSUMPTIONS

Finite element analyses (FEAs) were carried out using ABAQUS 6.17 [39]. The C3D8I solid elements (i.e., 8-node linear brick, incompatible mode) were used to discretize the models. To ensure a regular mesh, the structured-meshing technique was adopted, and a mesh sensitivity analysis was performed to select the mesh density (i.e., the number of finite elements per unit area) of the models, whose results in terms of von mises stress (VMS) at 6% of interstorey drift angle are summarized in Fig. 12. As it can be observed, the results are almost insensitive to the mesh size if the average dimension of the

Published in : Engineering Structures (2023), 116386
DOI: 10.1016/j.engstruct.2023.116386
Status : Postprint (Author's version)

finite elements is smaller than 12.5 mm, 10 mm, and 15 mm for the end-plate, the bolts and the beam-end, respectively. Therefore, these dimensions were used to discretize the FE models (see Fig. 13a).

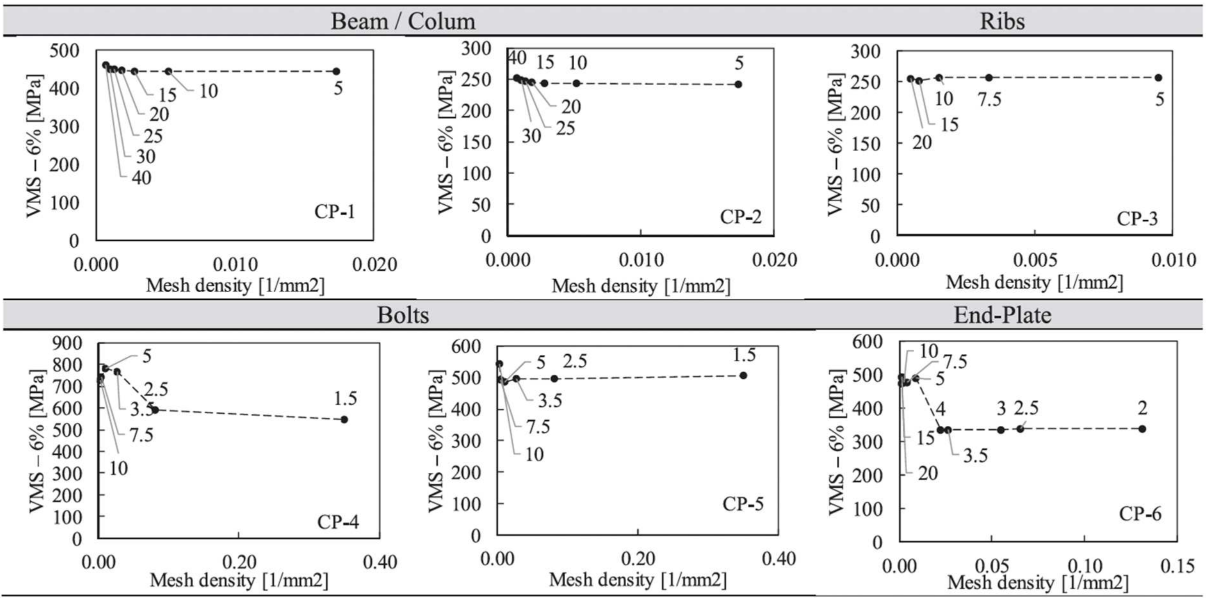

Fig. 12. Results of the mesh sensitivity analysis (the numbers of each solid dot indicate the average mesh size).

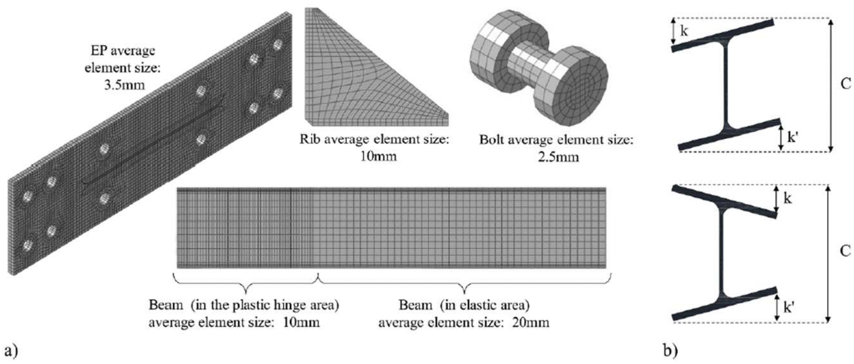

Fig. 13. Adopted mesh (a) and modelled beam imperfections (b).

The contacts were modelled by means of surface-to-surface interactions. In particular, "Hard Contact" formulation was used to simulate normal contact, and "Coulomb friction" was used to simulate the tangential behaviour assuming a friction coefficient equal to 0.3 (which corresponds to steel surfaces cleaned by wire-brushing with loose rust removed according to [1]).

The experimental properties of the materials were used (see Table 2) and true stress-true strain curves were derived from the experimental engineering curves. Von Misses yielding criterion was used together with combined (i.e., both isotropic and kinematic) plastic hardening.

The out-of-square imperfections of the flanges of steel members were considered by applying 80% of the maxima mill tolerances permitted by EN 10,034 [27], i.e., (k + k ')/C = 0.42% (see Fig. 13b). These imperfections were modelled by imposing the shapes of the related buckling Eigenmodes that were scaled to the considered amplitudes.

The bolts were modelled as dumbbell shapes (see Fig. 13a) to reduce the computational effort.

Published in : Engineering Structures (2023), 116386
DOI: 10.1016/j.engstruct.2023.116386
Status : Postprint (Author's version)

Therefore, their non-linear behaviour was simulated using the multilinear force-displacement curves given by [40,41] that were updated with measured material properties (see Table 2).

The pre-tensioning of bolts was modelled using the "Bolt load" option available in the software. The preload force was set equal to the actual value adopted to tighten the specimen (which was in accordance with [1]).

Full and fillet welds were modelled as solid elements with "Tie" constraints between the connected surfaces. The material of the welds was modelled as elastic perfectly plastic, with yield stress equal to 460 MPa [32].

The boundary conditions and torsional restraints were consistent with the sub-structuring shown in Fig. 4.

The analyses were performed in two steps, as follows: 1) application of the preloading in all bolts; 2) application of the experimental displacement histories at the tip of the beam using dynamic implicit solver with quasi-static options.

In Section 7.2, the FE results are shown and discussed in terms of predicted overall and local response curves and damage pattern, namely predicted failure mode and damage indexes, such as PEEQ (equivalent plastic strain index) and RI (rupture index). PEEQ is used to estimate the amount of plastic deformation in the damaged zones and is given by the following equation:

$$\mathrm{PEEQ} = \frac{\sqrt{\frac{2}{3}\varepsilon_{ij}^{p}\varepsilon_{ij}^{p}}}{\varepsilon_{y}} \tag{8}$$

where

$$\varepsilon_{ij}^{p} \text{ and } \varepsilon_{y}$$

are the tensor of plastic strains and uniaxial yield strain, respectively.

RI is used to compare the tendency to exhibit ductile rupture between different details of the same type of joint, as in [42–45], and is defined as follows:

$$RI = \frac{PEEQ}{exp(-1.5T)} = \frac{PEEQ}{exp\left(-1.5\frac{\sigma_m}{\sigma_e}\right)} \tag{9}$$

where σ_m and σ_e are the hydrostatic stress and Von Mises stress, respectively.

7.2. FE SIMULATIONS VS. EXPERIMENTAL RESULTS

Fig. 14 summarises the comparison between FE simulations and experimental results in terms of moment-rotation curves and failure mode. The distribution of equivalent plastic strains (PEEQ) is shown to highlight the location of plastic deformations. As it can be recognized, the finite element simulations satisfactory mimic the experimental response. In this regard, it is worth noting that the performed FE analyses aimed at investigating the local response of the tested joints, while the influence of the geometrical and mechanical features of the joints require a specific parametric study that is out of the scope of this article.

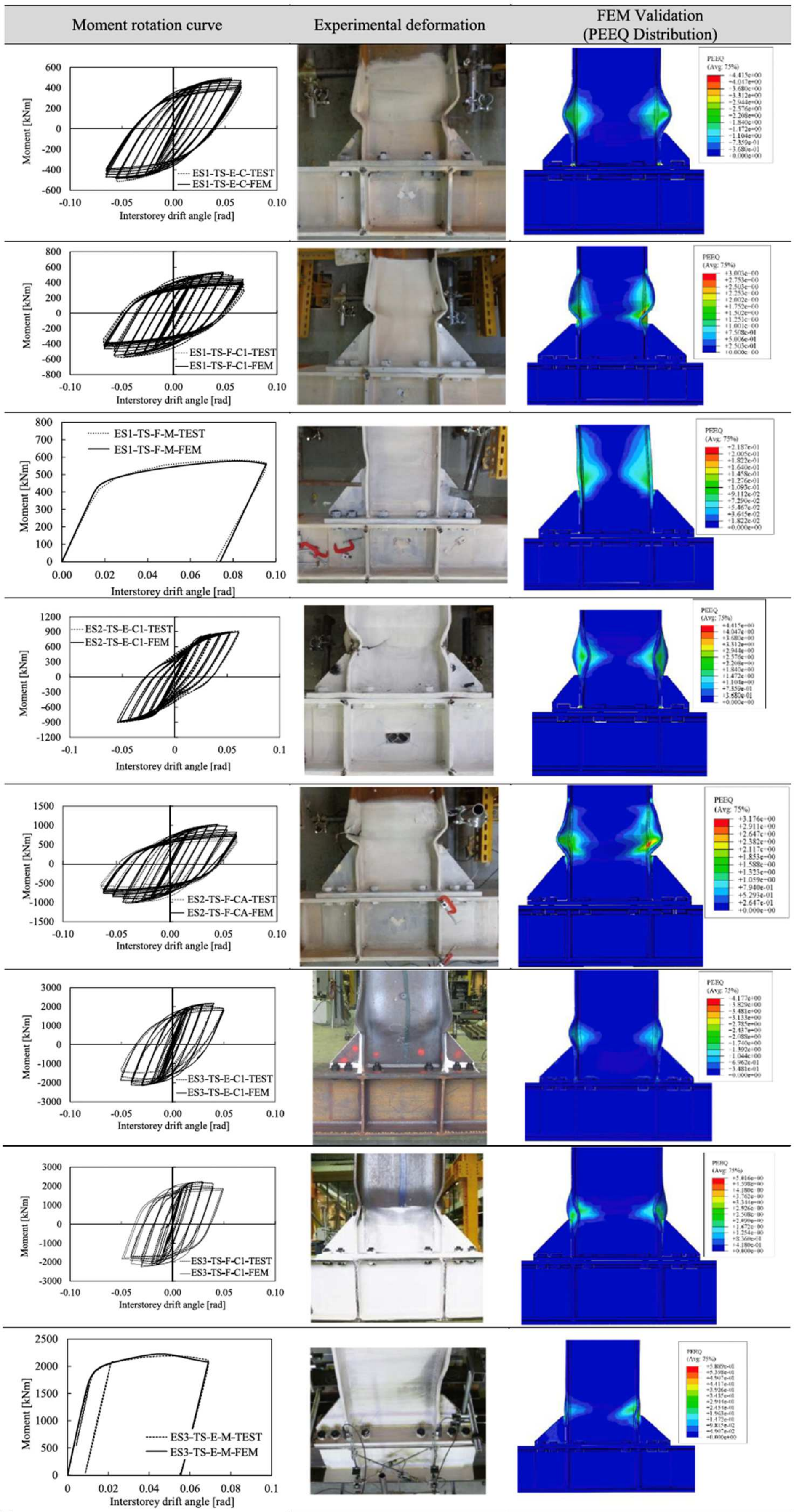

Fig. 14. FE simulations vs. experimental results.

Published in : Engineering Structures (2023), 116386
DOI: 10.1016/j.engstruct.2023.116386
Status : Postprint (Author's version)

Figs. 15 and 16 report the FE results of full and equal strength joints in terms of overall and local response. In both full and equal strength joints, the comparison between cyclic and monotonic responses highlights that the monotonic ductility of the joints is limited by the fracture of the bolts may fail at about 0.08 rad of intestorey drift angle due to the significant demand on the connection since the yielding zones (i.e., the beam plastic hinge for full strength joints and the end- plate in bending for the equal strength joints) do not deteriorate under monotonic loading. The compression forces (which were obtained by integrating the longitudinal normal stress) resulting in the web area of the rib (C_{Rib}) and the beam flange (C_{Flange}) at the end-plate interface are also depicted. As it can be observed, in case of full strength joints, these forces are comparable throughout the cyclic response of the joints, while in the case of equal strength joints, the C_{Flange} are about twice C_{Rib}, In all cases, the depth of the connected members does not appreciably influence the evolution of these forces. In addition, these forces influence the position of the center of compression (ξh_r) of the end-plate connection (being h_r the depth of the rib web) with respect to the centroid of the beam flange.

Published in : Engineering Structures (2023), 116386
DOI: 10.1016/j.engstruct.2023.116386
Status : Postprint (Author's version)

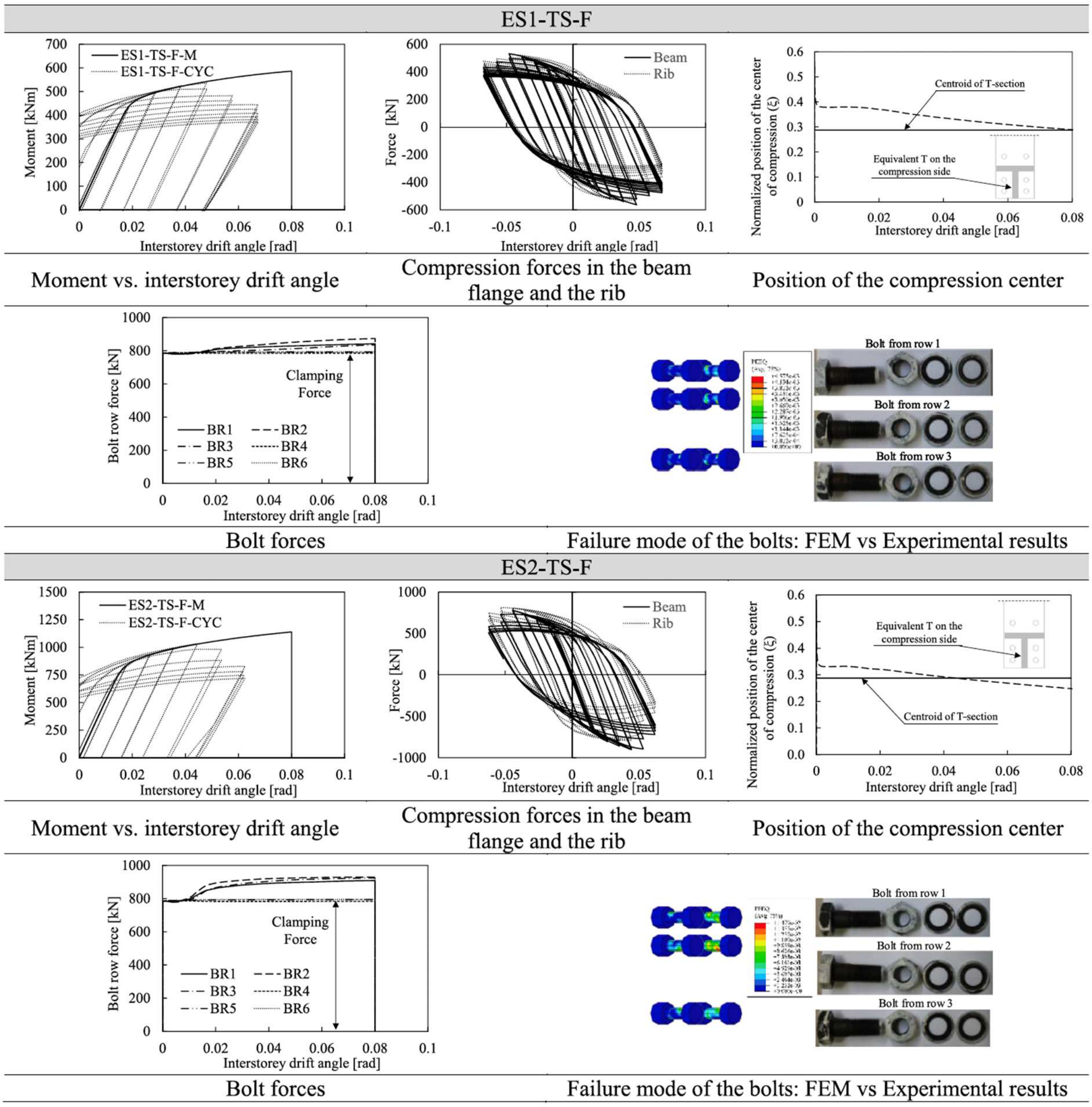

Fig. 15. Overall and local FE response of full strength joints.

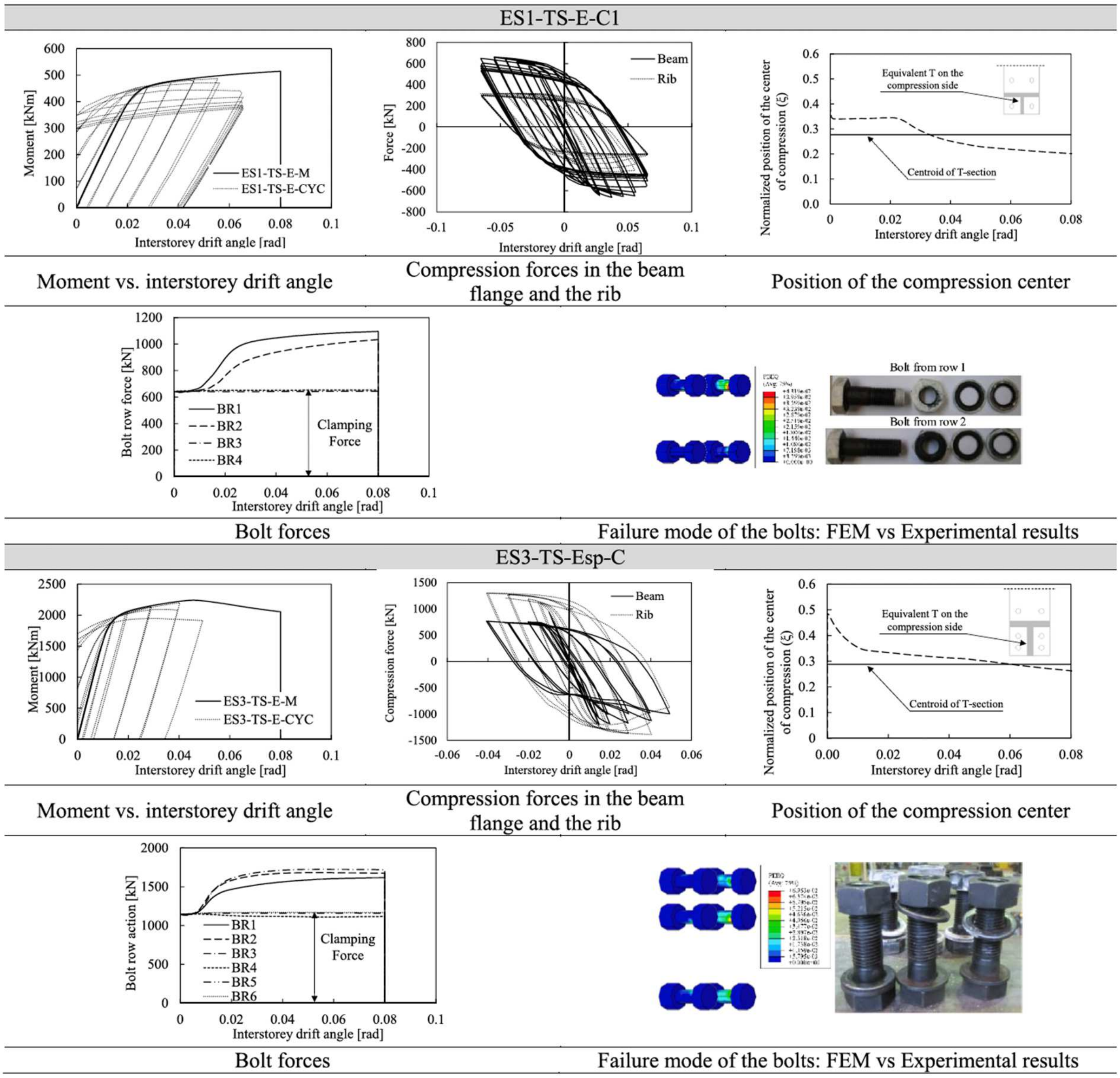

Fig. 16. Overall and local FE response of equal strength joints.

Figs. 15 and 16 also show the evolution of the normalized position of the center of compression (ξ) against the interstorey drift angle, where it can be observed that the design assumption that considers the centre of compression located in the centroid of the "T" area of the beam flange and the rib web is reasonable for the design performance of the joints at 0.04 rad, while it is rather conservative for smaller demand.

The evolution of tensile forces in the bolt rows is also depicted, showing that the design assumption considering active solely the bolt rows above (for the hogging moment) or below (for the sagging moment) the neutral axis of the beam is satisfactory. The distribution of PEEQ in the bolts shows that some negligible and localized plastic deformations also occur in the bolts in full strength joints, although no sign of damage was observed in the bolts after the experimental tests that were easily untightened. In the case of equal strength joints, the bolts fully yield at maximum drift angle as also confirmed by the after-test observations.

Fig. 17 shows the comparison between the simulated and the experimental damage pattern in the rib stiffener of the ES1 full strength joint (since the behaviour of the other tested joints is very similar). The measurements of the strain gauges confirmed that this stiffener behaves almost in the elastic range with the unique exception of the portion close to the rib toe, namely close to the plastic hinge of the beam. However, the measured strains (ε_{test}) slightly exceed the yield strain (ε_y) of the rib material (see Fig. 17a).

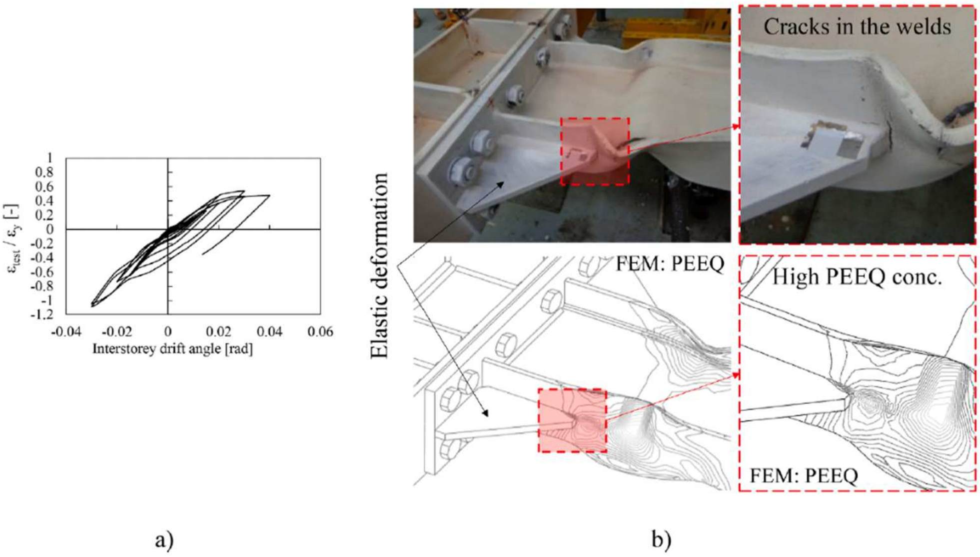

Fig. 17. Plastic deformations in the rib stiffener (ES1 full strength joint): a) measured strains (ε_{test}) normalized to yield strain (ε_y) at the tip of the rib vs. interstorey drift angle; b) experimental vs. simulated damage pattern.

It is also worth noting that the plastic demand mostly concentrates in the beam up to its capping rotation (i.e., the rotation corresponding to the peak bending moment); the deformation pattern in the ribs is almost constant. Following the beam buckling, the strain demand in the rib increases and, if the rib web remains in the elastic range, cracks occur at its toe (see Fig. 17b). Such results are also in line with what was observed by [44,46].

Fig. 18 depicts the distributions of RI across the flange width (b_f) at the beam flange to end plate weld toe which are plotted against the normalized position (x/b_f) of the measured five points of the beam width (i.e., the middle, half of mid-width and both edges) for 2%, 4% and 6% of interstorey drift angles. As it can be observed, RI is not greater than 1 up to 4% of interstorey drift angle, thus confirming a satisfactory performance in this range of overall demand. However, at 6%, RI is greater than 1 that implies tendency to develop fractures as also observed in the performed tests. In equal strength joints, RI increases with the beam depth, while full strength joints exhibit a different evolution of RI that is substantially greater in ES3 specimens. Therefore, it is evident a direct influence of the beam depth on RI, namely deeper beams may experience greater RI. This observation is also in line with the experimental results. In fact, the specimens with shallower beams (i.e., ES1 assemblies) were characterized by greater ductility.

Published in : Engineering Structures (2023), 116386
DOI: 10.1016/j.engstruct.2023.116386
Status : Postprint (Author's version)

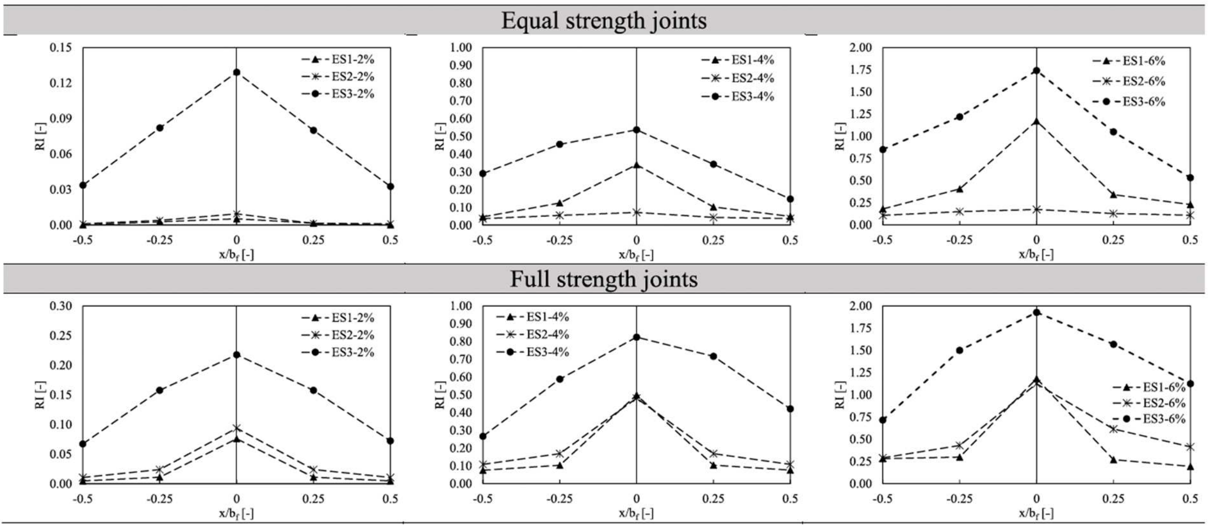

Fig. 18. Evolution of RI across the beam width.

8. Conclusions

This study summarizes the results of seismic prequalification tests of Extended Stiffened End-Plate (ESEP) joints in the framework of European codes (i.e., EN1998-1 and EN1993-1-8) for two different expected seismic performance, namely solely yielding of the beam (i.e., full strength joints) and balanced yielding of the beam and the end-plate of the bolted connection (i.e., equal strength joints). Design criteria and the technological details of the tested joints are presented, and results of finite element simulations are also shown. On the basis of the obtained results, the following conclusions can be drawn:

- Both full and equal strength joints exhibited ductile behaviour with a stable hysteretic response.
- The tests of full strength joints confirmed that plastic deformations mainly occurred in the beam plastic hinge that formed close to the toe of the rib stiffener. This failure mode is characterized by progressive strength degradation due to the local buckling of the beam.
- Equal strength joints exhibited a stable hysteretic response without strength degradation, because the plastic deformation is balanced between the end-plate in bending and the beam that did not pre-maturely buckle.
- In line with the design criteria, the column web panel of all tested joints remains in elastic range.
- The considered design over-strength factor for full strength connection (i.e., γ_{rm} x γ_{sh} = 1.25 x 1.2 = 1.5) ensured a satisfactory safety margin with the achievement of the expected failure mode of the joints. However, it is important to highlight that the measured values of the γ_{rm} x γ_{sh} from the performed tests are not exhaustive and cannot provide a definitive value about the overall design overstrength due to the limited number of specimens.
- The results of finite element analyses confirmed that the position of the centre of compression into the connection is in line with the design assumptions to estimate the lever arm of the connection at 0.04 rad of interstorey drift angle.

- Finite element simulations confirmed that the simplified assumptions on the active bolt rows in tension satisfactorily predict the response of the joints.
- The concentration of plastic deformations in the rib toe-to-beam weld explains the formation of cracks at the end of the tests. The rupture index increases with the beam depth, thus confirming the experimental evidence. Further experimental and numerical studies are necessary to investigate this problem and to enhance this tech- nological detail.

Déclaration of Competing Interest

The authors declare that they have no known competing financial interests or personal relationships that could have appeared to influence the work reported in this paper.

Data availability

The data are shared in the attached Annex.

Acknowledgments

The research activity presented in this paper received funding from the European Union's Research Fund for Coal and Steel (RFCS) research program under the following grant agreements:

- n° RFSR-CT-2013-00021- European pre-QUALified steel JOINTS: EQUALJOINTS;
- n° 754048 — EQUALJOINTS-PLUS — RFCS-2016.

Appendix A. Supplementary data

Supplementary data to this article can be found online at https://doi.org/10.1016/j.engstruct.2023.116386.

References

[1] EN 1993-1-8, Design of steel structures - Part 1-8: Design of joints.
[2] EN 1998-1, Design of structures for earthquake resistance - Part 1: General rules, seismic actions and rules for buildings.
[3] D'Aniello M, Landolfo R, Piluso V, Rizzano G. Ultimate Behaviour of Steel Beams under Non-Uniform Bending. J Constr Steel Res 2012;78:144-58. https://doi.org/ 10.1016/j.jcsr.2012.07.003.
[4] RFSR-CT-2007-00039. Optimizing the seismic performance of steel and steel concrete structures by standardizing material quality control (OPUS); 2013. ISBN: 978-92-79-29037-4. https://doi.org/10.2777/79330.

[5] Tartaglia R, D'Aniello M, Rassati GA, Swanson JA, Landolfo R. Full strength extended stiffened end-plate joints: AISC vs recent European design criteria. Eng Struct 2018;159:155-71. https://doi.org/10.1016/j.engstruct.2017.12.053.

[6] Tartaglia R, Zimbru M, D'Aniello M. Landolfo R, Finite element simulations on the ultimate response of extended stiffened end-plate joints. Steel and Composite Struct 2018;27(6):727-45. https://doi.org/10.12989/scs.2018.27.6.727.

[7] Tartaglia R, D'Aniello M, Landolfo R. The influence of rib stiffeners on the response of extended end-plate joints. J of Construct Steel Res 2018;148:669-90. https://doi.org/10.1016/j.jcsr.2018.06.025.

[8] Tartaglia R, D'Aniello M, Rassati GA. Proposal of AISC-compliant seismic design criteria for ductile partially-restrained end-plate bolted joints. J of Construct Steel Res 2019;159:364-83. https://doi.org/10.1016/j.jcsr.2019.05.006.

[9] Guo B, Gu Q, Liu F. Experimental behavior of stiffened and unstiffened end-plate connections under cyclic loading. J Struct Eng 2006;132(9):1352-7.

[10] Shi Y, Shi G, Wang Y. Experimental and theoretical analysis of the moment-rotation behaviour of stiffened extended end-plate connections. J Constr Steel Res 2007;63(9):1279-93.

[11] Lee C-H. Seismic design of rib-reinforced steel moment connections based on Equivalent Strut Model. J Struct Eng ASCE 2002;128(9):1121-9.

[12] Abidelah A, Bouchaïr A, Kerdal DE. Experimental and analytical behavior of bolted end-plate connections with or without stiffeners. J Constr Steel Res 2012;76:13-27.

[13] Lee C-H, Jung J-H, Oh M-H, Koo E-S. Experimental study of cyclic seismic behavior of steel moment connections reinforced with ribs. J Struct Eng ASCE 2005;131(1): 108-18.

[14] Ghobarah A, Korol RM, Osman A. Cyclic behavior of extended end-plate joints. J Struct Eng 1992;118:1333-11135.

[15] Ghobarah A, Osman A, Korol RM. Korol, Behaviour of extended end-plate connections under cyclic loading. Eng Struct 1990;12(1):15-27.

[16] Nogueiro P, Simoes da Silva L, Bento R, Simoes R. Experimental behavior of standardized European end-plate beam-to-column steel joints under arbitrary cyclic loading, Proceeding of Stability and ductility of steel structures. Lisbon, Portugal, September 6-8. 2006.

[17] Sumner EA, Murray TM. Behaviour of Extended End-Plate Moment Connections Subject to Cyclic Loading. J of Struct Eng 2008;128(4):501-8.

[18] Mahin S, Malley J, Hamburger R. Overview of the FEMA/SAC program for reduction of earthquake hazards in steel moment frame structures. J Construct S Res 2002;58(5-8):511-28.

[19] AISC (American Institute of Steel Construction), Seismic Provisions for Structural Steel Buildings, ANSI/AISC 341-16, Chicago, IL; 2016.

[20] AISC (American Institute of Steel Construction), Prequalified Connections for Special and Intermediate Steel Moment Frames for Seismic Applications, ANSI/ AISC 358-16, Chicago, IL; 2016.

[21] Building Standard of Law in JAPAN (BSL). Japanese Minister of land, infrastructure and transportation; 2013.

[22] Architectural Institute of Japan. Recommendation for Design of Connections in Steel Structures. Tokyo: Maruzen Publishing Co., Ltd.; 2012. in Japanese.

[23] Murray TM. AISC design guide 4. Extended end-plate moment connections. Chicago, IL: AISC (American Institute of Steel Construction); 1990.

Published in : Engineering Structures (2023), 116386
DOI: 10.1016/j.engstruct.2023.116386
Status : Postprint (Author's version)

[24] Sumner EA, Murray TM. Performance of extended moment end-plate connections subject to seismic loading. U.S.-Japan Workshop on Seismic Fracture Issues in Steel Structures, San Francisco, California, February 28-March 1; 2000.

[25] Sumner EA, Murray TM. Behavior of extended end-plate moment connections subject to cyclic loading. J Struct Eng-ASCE 2002;128(4):501-8.

[26] Murray TM, Sumner EA. AISC design guide 4. Extended end-plate moment connections—seismic and wind applications. 2nd ed. Chicago, IL: AISC (American Institute of Steel Construction); 2004.

[27] CEN 1993. CEN (European Committee for Standardization). Structural steel I and H sections: tolerances on shape and dimensions. EN 10034, Brussels; 1993.

[28] ASTM (American Society for Testing and Materials International). Standard specification for general requirements for rolled structural steel bars, plates, shapes, and sheet piling. ASTM A6/A6M, West Conshohocken, PA; 2016.

[29] Landolfo R. (2022) European seismic prequalification of steel beam-to-column joints: EQUALJOINTS and EQUALJOINTS-Plus projects. J Constr Steel Res 2022; 192:107238. DOI: 10.1016/j.jcsr.2022.107238.

[30] D'Aniello M, Tartaglia R, Costanzo S, Landolfo R. Seismic design of extended stiffened end-plate joints in the framework of Eurocodes. J Constr Steel Res 2017; 128:512-27. https://doi.org/10.1016/j.jcsr.2016.09.017.

[31] CEN/TC250/SC8, prEN 1998-1-2 Eurocode 8: — Design of structures for earthquake resistance — Part 1-2: Rules for new buildings.

[32] ISO 14341:2020 - Welding consumables. Wire electrodes and weld deposits for gas shielded metal arc welding of non alloy and fine grain steels. Classification.

[33] EN 1090-2: Execution of steel Structures and aluminium structures. Part 2: Technical requirements for steel structures; 2011.

[34] Dubina D, et al. High strength steel in seismic resistant building frames (HSS- SERF), Commission Europeenne; 2015. ISBN: 978-92-79-44081-6. (DOI: 10.2777/ 725123).

[35] Ballio G, Calado L, De Martino A, Faella C, Mazzolani FM. Cyclic behaviour of steel beam-to-column joints experimental research. Costruzioni Metalliche 1987;2: 69-90.

[36] Mele E, Calado L, De Luca A. Experimental investigation on European welded connections. J Struct Eng (ASCE) 2003;129(10):1301-11.

[37] Araujo M, Macedo L, Castro JM. Evaluation of the rotation capacity limits of steel members defined in EC8-3. J Constr Steel Res 2017;135:11-29.

[38] Zhao H, Shi G, Chen X, Xiao T. Finite element analysis and design of retrofitted beam-to-column joints with welded haunches. J Constr Steel Res 2021;186: 106924. https://doi.org/10.1016/j.jcsr.2021.106924.

[39] Systemes D. Abaqus analysis 6.14 user's manual. Simulia Inc.; 2015.

[40] D'Aniello M, Cassiano D, Landolfo R. Monotonic and cyclic inelastic tensile response of European preloadable GR10.9 bolt assemblies. of Construct. Steel Res h 2016;124:77-90. https://doi.org/10.1016/j.jcsr.2016.05.017.

[41] D'Aniello M, Cassiano D. Landolfo R, Simplified criteria for finite element modelling of European preloadable bolts. Steel Compos Struct, Int J 2017;24(6): 643-58. https://doi.org/10.12989/scs.2017.24.6.643.

[42] Ricles JM, Fisher JW, Lu LW, Kaufmann EJ. Development of improved welded moment connections for earthquake-resistant design. J Constr Steel Res 2002;58 (5):565-604.

Published in : Engineering Structures (2023), 116386
DOI: 10.1016/j.engstruct.2023.116386
Status : Postprint (Author's version)

[43] Hancock JW, Mackenzie AC. On the mechanisms of ductile failure in high strength steels subjected to multi-axial stress states. J Mech Phys Solids 1976;24(2-3): 147-60.

[44] Trevor Szabo, Matthew R. Eatherton, Xiuzhang He, Thomas M. Murray. Study of a twelve bolt extended stiffened end-plate moment connection. Report No. CE/VPI- ST-17/02, Virginia Polytechnic Institute and State University; 2017.

[45] Morrison M, Quayyum S, Hassan T. Performance enhancement of eight bolt extended end-plate moment connections under simulated seismic loading. Eng Struct 2017;151(2017):444-58.

[46] Cermelj B, Moze P, Sinur F. On the prediction of low-cycle fatigue in steel welded beam-to-column joints. J Constr Steel Res 2016;117:49-63. https://doi.org/ 10.1016/J.JCSR.2015.09.017.

[47] Francavilla AB, Latour M, Piluso V, Rizzano G. Design of full-strength full-ductility extended end-plate beam-to-column joints. Journal of Constructional Steel Research 2018;148:77-96.

[48] Iannone F, Latour M, Piluso V, Rizzano G. Experimental analysis of bolted steel beam-to-column connections: Component identification. Journal of Earthquake Engineering 2011;15(2):214-44.

[49] Latour M, Piluso V, Rizzano G. Cyclic modeling of bolted beam-to-column connections: Component approach. Journal of Earthquake Engineering 2011;15 (4):537-63.